2018

Carbon and Nitrogen Isoscapes in West Antarctica Reflect Oceanographic Transitions

Emily K. Brault

Paul L. Koch

Kelton W. McMahon
University of Rhode Island, kelton_mcmahon@uri.edu

Kyle H. Broach

Aaron P. Rosenfield

See next page for additional authors

Citation/Publisher Attribution

Brault, E. K., Koch, P. L., McMahon, K. W., Borach, K. H., Rosenfield, A. P., Sauthoff, W., Loeb, V. J.,...Smith, W. O., Jr. (2018). Carbon and Nitrogen Isoscapes in West Antarctica Reflect Oceanographic Transitions. *Marine Ecology Progress Series, 593,* 29-45. doi: 10.3354/meps12524.
Available at: https://doi.org/10.3354/meps12524

Carbon and Nitrogen Isoscapes in West Antarctica Reflect Oceanographic Transitions

Emily K. Brault[1,*], Paul L. Koch[2], Kelton W. McMahon[3], Kyle H. Broach[2], Aaron P. Rosenfield[2], Wilson Sauthoff[1], Valerie J. Loeb[4], Kevin R. Arrigo[5], Walker O. Smith Jr[6]

[1]Department of Ocean Sciences, University of California, Santa Cruz, CA 95064

[2]Department of Earth and Planetary Sciences, University of California, Santa Cruz, CA 95064

[3]Graduate School of Oceanography, University of Rhode Island, Narragansett, RI 02882

[4]Moss Landing Marine Laboratories, Moss Landing, CA 95039

[5]Department of Earth System Science, Stanford University, Stanford, CA 94305

[6]Virginia Institute of Marine Science, College of William and Mary, Gloucester Point, VA 23062

*ebrault@ucsc.edu

ABSTRACT: Antarctic marine ecosystems are spatially and temporally dynamic. Regional climate change is significantly altering the patterns and magnitudes of this dynamism with cascading impacts on biogeochemistry, productivity, and food web architecture. Isoscapes (or isotopic maps) provide a valuable analytical framework to characterize ecosystem processes and address questions about trophic dynamics, animal movement, and elemental cycling. Applications of stable isotope methods to Antarctic ecosystems are currently limited by a paucity of information on geospatial isotope characteristics within the Southern Ocean. In response, we have created the first empirically derived zooplankton isoscapes for West Antarctica based on analysis of bulk nitrogen (N) and carbon (C) isotope values ($\delta^{15}N$ and $\delta^{13}C$, respectively) in 94 zooplankton specimens from the Drake Passage, West Antarctic Peninsula (WAP), and Amundsen and Ross Seas. The zooplankton $\delta^{15}N$ values increased by 3 ‰ from north of the Polar Front (3.3 ± 0.6 ‰) to the Ross Sea (6.2 ± 0.8 ‰), reflecting a productivity gradient across this region. Abundant open water polynyas in the Amundsen and Ross Seas exhibit strong nitrate drawdown, resulting in more ^{15}N-enriched phytoplankton and zooplankton relative to those from the generally less productive WAP and Drake Passage. Zooplankton $\delta^{13}C$ values decreased by 3 ‰ from north of the Polar Front (-24.2 ± 0.9 ‰) to the Ross Sea (-27.5 ± 1.6 ‰), likely driven by decreasing sea surface temperatures with increasing latitude. Our isoscapes are a valuable first step in establishing isotopic spatial patterns in West Antarctica and are critical for addressing numerous ecosystem questions.

KEYWORDS: Isoscape, Antarctica, Zooplankton, Biogeochemistry, Animal migration, Food web, ENSO

INTRODUCTION

The Southern Ocean is one of the largest, most dynamic ecosystems on Earth, playing a critical role in ocean primary productivity and fisheries production, biogeochemical cycling, and global climate (Falkowski et al. 1998, Gille 2002, Croxall & Nicol 2004, Marinov et al. 2006). It consists of the waters south of the Subtropical Front, including the Antarctic Circumpolar Current (ACC) and high latitude waters surrounding the Antarctic continent. West Antarctica, the Southern Ocean region between the Ross and Weddell Seas, is experiencing some of the most profound and rapid regional climate change on Earth (Meredith & King 2005, Ducklow et al. 2007, 2012, Stammerjohn et al. 2012). Warming is predicted to result in increased upper ocean stratification and altered phytoplankton assemblages with unknown long-term ecosystem consequences (Arrigo et al. 2000, Jacobs et al. 2002, Tortell et al. 2008). Climate change impacts on a range of taxa have been documented in the Southern Ocean over the past 50 years, including phytoplankton (Montes-Hugo et al. 2009), Antarctic krill and other pelagic invertebrates at the base of the food web (Atkinson et al. 2004), and upper trophic level consumers, including sea birds, penguins, and marine mammals (Trathan et al. 2007, Nicol et al. 2008, Siniff et al. 2008, Forcada & Trathan 2009). Given the rapid physical, chemical, and biological changes occurring in West Antarctica, it is critical to understand the underlying biogeochemical cycling that supports the base of Antarctic food webs and ultimately controls the ecological response to climate change.

Stable isotope analysis is now a routine tool to characterize elemental cycling and trophic dynamics (Boecklen et al. 2011). Stable nitrogen (N) isotope values ($\delta^{15}N$) are typically used to determine the number of trophic transfers between a consumer and the base of the food web, while stable carbon (C) isotope values ($\delta^{13}C$) are often used to infer sources of primary production fueling food webs (Peterson & Fry 1987). Ecological applications of stable isotope data, termed ecogeochemistry, require careful consideration of the spatio-temporal dynamics of isotope values at the base of the food web (Graham et al. 2010, McMahon et al. 2013a).

Geospatial maps of isotopic values, termed isoscapes, provide an analytical framework for understanding regional biogeochemical processes (Bowen 2010, West et al. 2010, McMahon et al. 2013a). Isoscapes generated from organisms at the base of the food web provide an integrated view of the spatial gradients in stable isotope values within a system. A number of factors can influence baseline stable nitrogen isotope ($\delta^{15}N_{baseline}$) and carbon isotope ($\delta^{13}C_{baseline}$) values (Wainwright & Fry 1994, Needoba et al. 2003, Montoya 2007,2008, Chikaraishi et al. 2009, Graham et al. 2010). For instance, phytoplankton $\delta^{15}N$ values are set by their nutrient source (i.e., nitrate, ammonium, or N_2), biological transformations (e.g., N_2-fixation and denitrification), isotopic fractionation during N assimilation, and nutrient pool size (or the extent of nitrogen pool drawdown) (reviewed in McMahon et al. 2013a). For carbon, variability in the $\delta^{13}C$ value of phytoplankton reflects dissolved inorganic carbon $\delta^{13}C$ values, $[CO_2]_{aq}$, temperature, cell size and geometry, internal biological parameters (e.g., growth rate), and CO_2 drawdown (reviewed in McMahon et al. 2013a). Spatial and temporal variations in these driving forces (e.g., seasonal or latitudinal gradients in temperature) will in turn create spatial and temporal variations in phytoplankton isotope values (e.g., Schell et al. 1998). Phytoplankton $\delta^{15}N$ and $\delta^{13}C$ values at the base of the food web are subsequently passed on, with modifications associated with trophic transfer, to upper trophic level consumers (e.g., Lorrain et al. 2009, Graham et al. 2010, Jaeger et al. 2010a).

In recent years, researchers have established baseline isoscapes for a number of regions and spatial scales (e.g., McMahon et al. 2013a, MacKenzie et al. 2014, Vokhshoori et al. 2014, Vokhshoori & McCarthy 2014), and these efforts have produce profound insights into animal movement and foraging ecology, habitat use, and regional biogeochemical cycling (e.g., Graham et al. 2010, Jaeger et al. 2010b, MacKenzie et al. 2011). The Southern Ocean has the potential for significant geospatial isotope dynamics, which would facilitate similar studies in this critical ecosystem. Four major fronts separate the Southern Ocean into five distinct biogeographic zones (from north to south): the Subtropical Zone (STZ), Subantarctic Zone (SAZ), Polar Front Zone (PFZ), Antarctic Zone (AZ), and Antarctic Continental Zone (ACZ) (Fig. 1). Baseline isotope values have not yet been determined for all major frontal zones and seas, such as the Amundsen and Ross Seas in the Pacific Sector. Where available, isotopic baselines are proving useful in interpreting broad ecosystem dynamics.

Off East Antarctica (the portion of the continent largely within the Eastern Hemisphere), DiFiore et al. (2006) have determined summer and winter $\delta^{15}N_{NO3-}$ values for the STZ, SAZ and PFZ. They describe a seasonal increase in surface water of $\delta^{15}N_{NO3-}$ values in surface waters, which are greatest in the summer and associated with a decrease in NO_3^- concentration [NO_3^-]. The authors attribute the inverse relationship between $\delta^{15}N_{NO3-}$ value and [NO_3^-] and the resulting seasonal pattern in $\delta^{15}N_{NO3-}$ values to phytoplankton NO_3^- consumption, which increases the $\delta^{15}N$ value of the residual NO_3^- pool. DiFiore et al. (2006) also report decreasing surface water $\delta^{15}N_{NO3-}$ values with increasing latitude from ~ 13.5 ‰ at 42 °S to ~ 7.5 ‰ at 54 °S, which may have resulted from decreasing productivity between the STZ and PFZ. DiFiore et al. (2009) also measured $\delta^{15}N_{NO3-}$ values at three regions along the East Antarctic continental margin and in the Ross Sea polynya, all sites within the ACZ and at latitudes between about 65 °S and 80 °S. The authors report surface water $\delta^{15}N_{NO3-}$ values ranging from about 5 ‰ to 8 ‰, with the highest values at productivity "hot spots" that have the highest surface NO_3^- depletions.

The surface water $\delta^{15}N_{NO3-}$ values of hot spot locations are similar to those measured in the PFZ at ~ 54 °S, conflicting with prior work suggesting a consistent decrease in $\delta^{15}N_{NO3-}$ with increasing latitude (DiFiore et al. 2006). Somes et al. (2010) used a marine ecosystem model with N isotopes to construct a global map of $\delta^{15}N_{NO3-}$ values, which they compare to a global database of $\delta^{15}N_{NO3-}$ values. From their model, $\delta^{15}N_{NO3}^{-}$ values decrease with increasing latitude in the Southern Ocean, likely due to increasing [NO_3^-] (Somes et al. 2010). Jaeger et al. (2010a) defined the isotopic baseline in open waters of the southwest Indian Ocean by measuring isotopic values in the feathers of seabirds. They report decreases in both $\delta^{15}N$ (12.9 ‰ to 8.2 ‰) and $\delta^{13}C$ (-19.0 ‰ to -23.7 ‰) values of light-mantled sooty albatross (*Phoebetria palpebrata*) from the STZ towards the AZ.

Despite the potential for strong isotope gradients in the West Antarctic and the clear value of quantifying and understanding regional geospatial isotope dynamics here, there have been no isoscapes generated for this critical region. This is particularly troubling given that the rapid warming and associated ecological and environmental changes this system is experiencing. In this study, we generate the first empirical isoscapes for the West Antarctic region by measuring the $\delta^{15}N$ and $\delta^{13}C$ values of multiple taxa of zooplankton and phytoplankton taxa. These isoscapes cover an expansive area of the West Antarctic: from the tip of South America to the Antarctica Peninsula, and along the West Antarctic coast from the Peninsula to the Ross Sea. This study focuses on isoscapes of West Antarctic continental margins because these systems are ecologically critical zones for fisheries, seabirds, and marine mammals and have not been fully assessed in prior isoscapes. The isoscapes generated in this study will serve as an important first step to quantifying the geospatial isotope dynamics of this critical ecosystem and understanding the underlying mechanisms generating these patterns. Our work also highlights key gaps in data needed to realize the full potential of this powerful isotope approach to understanding movement, foraging ecology, and biogeochemical cycling in the Southern Ocean. In particular, we discuss the need for additional research to carefully examine temporal variability in isotopic baselines as a result of physical conditions fluctuating across seasons and climate modes, as well as to increase the data coverage in certain West Antarctic regions, such as the Bellinghausen Sea. This work not only provides an initial framework for understanding baseline variability in Antarctic food webs, past and present, but also serves as a benchmark for evaluating future ecological and biogeochemical changes associated with rapid climate change.

MATERIALS AND METHODS

Sampling Sites

Plankton samples were collected between 2007 and 2015 adjacent to shore over the continental shelves in the ACZ of the West Antarctic Peninsula (WAP), Amundsen Sea, and Ross Sea, as well as from open water off the continental shelf in the AZ and from the PFZ and SAZ between the WAP and South America (Fig. 1). Ninety-four discrete samples, comprising a variety of zooplankton taxa (average of four taxa per station; Table S1), were collected at 34 stations over this region, including: five stations across the PFZ and SAZ waters, five stations within the AZ, ten nearshore stations off the WAP in the ACZ, seven stations in the Amundsen Sea, and seven stations in the Ross Sea.

Within the Palmer Long-Term Ecological Research (PAL-LTER) study area along the WAP and on the continental shelf, phytoplankton and Antarctic krill were collected during austral summers between 2007 and 2011: phytoplankton, December and January of 2009/10 and 2010/11 and krill, January of 2007/08 and 2010/11. We incorporate $\delta^{15}N$ and $\delta^{13}C$ values of

PAL-LTER krill samples reported in Brault (2012) into our isoscapes. Amundsen and Ross Sea zooplankton and phytoplankton were collected on the 2007/08 and 2010/11 *RV Oden* austral summer (December to January) cruises. All Ross Sea samples were obtained on the continental shelf. For the Amundsen Sea samples, four samples were collected on the continental shelf and the other three samples were collected within the continental margin. Zooplankton samples were taken from the ACZ, AZ, PFZ and SAZ during the early austral fall (March to April) 2015 cruise of the *SV Lawrence M. Gould*. Of these samples, only sampling within the ACZ was on the continental shelf. Mixed phytoplankton and zooplankton samples were obtained from the western Ross Sea during the 2011/2012 austral summer (January to February) cruise of the *RV Nathaniel B. Palmer*. All samples in this region were from sites on the continental shelf.

Sample Collection

Phytoplankton samples from the PAL-LTER surveys were collected using an 80 µm ring net towed through the upper water column (≤ 50 m depth) for ~ 30 minutes. The phytoplankton sample was rinsed into a pre-cleaned plastic tub, re-concentrated by sieving through a 25 µm mesh, and then frozen at -80 °C. A sub-sample of each tow was examined under a compound microscope to determine the dominant species (diatoms in all cases) and any microzooplankton were removed manually. Phytoplankton were collected during the *Oden* cruises of 2007/08 and 2010/11 via vertical tows from depths of ~ 20 m with a 30 µm ring net. Samples were similarly re-concentrated and frozen at -80 °C. The 2010/11 samples were determined to be dominated by the prymnesiophyte *Phaeocystis antarctica* according to onboard microscopy of tow sub-samples and once again any microzooplankton were discarded manually. The 2007/08 samples were not evaluated under a microscope to identify the dominant phytoplankton species.

Krill obtained during the PAL-LTER sampling, mixed zooplankton samples collected during the *Oden* cruise in 2010/11, and one sample of *Clione limacina* from a 2007/08 *Oden* cruise were derived from oblique tows (700 µm square-frame net) in 120 m and 400 m water depth for PAL-LTER and *Oden* cruises, respectively. Samples were transferred from the cod end into pre-cleaned buckets, re-concentrated by sieving through 700 µm mesh (retaining the retentate), and frozen at -80 °C. Samples were identified to the lowest taxonomic group possible prior to freezing. Zooplankton samples from the *L. M. Gould* cruise were obtained with open oblique hauls of a 505 µm mesh net from ~ 150 m to the surface using a 1.8 m Isaacs-Kidd midwater trawl. Samples were filtered through a 505 µm mesh sieve, sorted by species, and frozen at -20 °C. Mixed phytoplankton and zooplankton samples from the 2011/2012 cruise aboard the *RV Nathaniel B. Palmer* were collected with 200 µm bongo net tows in the upper water column (0-200 m). The samples were stored in a 4 % formaldehyde-seawater mixture at 4 °C.

Taxonomic Groups

All of the phytoplankton samples were treated together as "phytoplankton". Zooplankton taxonomic categories from the Ross and Amundsen Seas were (1) copepods, (2) gammarid and hyperiid amphipods, (3) euphausiids (larval, juvenile, adult), (4) *Salpa thompsoni*, and (5) pteropods *Clione limacina* (naked) and *Limacina helicina* (shelled) (Table S1). The WAP and Drake Passage samples consisted of euphausiid species *E. superba, E. crystallorophias, E. frigida, E. triacantha* and *Thysanoessa macrura*, hyperiid amphipod species *Themisto gaudichaudii*, *Vibilia antarctica* and *Primno macropa, Salpa thompsoni* and the pteropod *Spongiobranchia australis* (naked) (Table S1).

Sample Preparation

All samples were kept frozen until laboratory preparation, except for the formaldehyde-preserved plankton samples. Phytoplankton collected on the *Oden* cruises and phytoplankton and krill from the PAL-LTER cruises were freeze-dried at the Virginia Institute of Marine Science (VIMS, Gloucester Point, VA) with a Labconco Freezone Plus 6 at -80 ˚C for ~ 72 hours. Krill were homogenized with a Virtis "45" tissue homogenizer (Virtis Co., Inc.) before freeze-drying. Phytoplankton samples were manually homogenized after freeze-drying. Zooplankton from the *Oden* and *L. M. Gould* cruises, sorted by taxon at each station were freeze-dried at the University of California, Santa Cruz (UCSC) using a Labconco Freeze Dry System (Lyph Lock 4.5) at -40 ˚C for ~ 48 hours and then manually homogenized. All freeze-dried phytoplankton and zooplankton samples were stored in a dessicator after drying.

Sub-samples of all zooplankton samples were lipid-extracted, except for the Antarctic shelled-pteropods, to account for lipid ^{13}C-depletion relative to other biochemical classes. Lipid removal decreased atomic C:N ratios by about two for zooplankton. We note that a few specimens for two taxa have anomalously high atomic C:N ratios for lipid-free material (Table S1). The effect of chitin content on $\delta^{15}N$ and $\delta^{13}C$ values is poorly understood, but given zooplankton chitin contents (Ventura et al. 2006) and isotopic offsets between protein and chitin (Perkins et al. 2013), the presence of chitin in whole zooplankton material may result in lower $\delta^{15}N$ values and higher $\delta^{13}C$ values by up to about 2 ‰ and 1 ‰, correspondingly, relative to those of pure protein. Since the magnitude of the chitin content effect on $\delta^{15}N$ and $\delta^{13}C$ values is uncertain and such an effect would either be negligible or amplify our observed pattern, we have not removed zooplankton data with anomalously high atomic C:N ratios from our analyses.

Carbonate shells of the pteropod *Limacina helicina* were acidified and decarbonated with a 10% HCl solution. After HCl treatment, the samples were neutralized with Milli-Q water

(Thermo Fisher Scientific, Inc.) and freeze-dried in the UCSC Labconco Freeze Dry System as described above. These samples were not lipid-extracted due to sample size limitations but are considered lipid-poor (Kattner et al. 1998).

The PAL-LTER krill were lipid-extracted at the VIMS over three days using a chloroform:methanol (1:2; v:v) mixture via Soxhlet extraction (Bligh & Dyer 1959). After lipid extraction, samples were dried and frozen at -80 ˚C until stable isotope analysis. While non-lipid extracted material was not retained for $\delta^{15}N$ analysis, we found no significant difference in the $\delta^{15}N$ value of the lipid-extracted and lipid-inteact krill from PAL-LTER. A portion of each zooplankton sample from the *Oden* and *L. M. Gould* cruises was lipid-extracted via Accelerated Solvent Extraction (1500 psi; 60 ˚C; 3 cycles) with petroleum ether, according to a lab-established protocol at the UC Santa Cruz (Dobush et al. 1985, Kurle et al. 2002). For these zooplankton samples, $\delta^{13}C$ values were obtained from lipid-extracted material and $\delta^{15}N$ values were obtained from the non-extracted material.

To remove the formaldehyde-seawater solution from the Ross Sea mixed plankton samples, samples were transferred to 50 ml BD Falcon centrifuge tubes, centrifuged (15 min, 10,000 rpm), and decanted. The pellet was rinsed with Milli-Q water and centrifuged (15 min, 10,000 rpm) three times, discarding the supernatant between rinses. Samples were then transferred to 10 ml borosilicate vials and dried at 60 ˚C. We acknowledge that prior research has shown that formalin-preservation may affect $\delta^{15}N$ and $\delta^{13}C$ values (Sarakinos et al. 2002, González-Bergonzoni et al. 2015). From analysis of fish tissues, González-Bergonzoni et al. (2015) suggest that the formalin preservation effect (4 % formalin solution) on $\delta^{15}N$ values is ecologically insignificant relative to the range of values in our system. Formalin-fixed $\delta^{13}C$ values were ~ 0.9 ‰ less than those of fresh material. Since formalin may affect isotope values, we produced separate nitrogen and carbon isoscapes for the formalin-preserved samples in this study (Table S2).

Isotopic Analysis

For $\delta^{15}N$ and $\delta^{13}C$ analyses, ~ 1 mg of samples were weighed into tin cups (Costech, 3×5 mm) for elemental analysis-isotope ratio mass spectrometry (EA-IRMS). The PAL-LTER krill were analyzed at VIMS on a Costech ECS 4010 CHNS-O Elemental Analyzer (EA) (Costech Analytical Technologies, Inc.) coupled to a Delta V Advantage Isotope Ratio Mass Spectrometer (IRMS) with a Conflo IV Interface (Thermo Electron North America, LLC). The $\delta^{15}N$ and $\delta^{13}C$ values were referenced to AIR and V-PDB standards, respectively. Blanks and international standards – USGS 40 (L-glutamic acid with $\delta^{15}N$ and $\delta^{13}C$ values of -4.5 ‰ and -26.4 ‰, respectively) and USGS 41 (enriched L-glutamic acid with ^{15}N and $\delta^{13}C$ values of 47.6 ‰ and 37.6 ‰, correspondingly) – were analyzed on the EA-IRMS after every ten samples (standard deviations were < 0.1 ‰ for both $\delta^{15}N$ and $\delta^{13}C$). All other phytoplankton and zooplankton samples were analyzed at the Stable Isotope Lab at UC Santa Cruz using a Carlo Erba EA 1108 EA coupled to a Thermo-Finnigan Delta^{Plus} XP IRMS referenced to AIR and V-PDB standards for N and C, respectively. We applied mass and drift corrections during each instrument session with analysis of gelatin standard replicates. Standard deviations for standards were < 0.1 ‰ for both $\delta^{15}N$ and $\delta^{13}C$ (seven standards analyzed at the start of each session and a standard analyzed after every eight samples during the session).

Data Analyses

Analyses of spatial patterns in the $\delta^{15}N$ and $\delta^{13}C$ values of phytoplankton and zooplankton taxa were performed with Ocean Data View (ODV) version 4.7.4 (Schlitzer 2015) using Data Interpolating Variational Analysis (DIVA) gridding software (Barth et al. 2010).

DIVA gridding is highly optimized and relies on a finite-element resolution that takes into account the distance between analysis and data (observation constraint), the regularity of the analysis (smoothness constraint) and physical laws (behavior constraint). DIVA also takes into account coastlines, sub-basins, and advection. Color-shaded contour maps were produced to display $\delta^{15}N$ and $\delta^{13}C$ values using DIVA gridding for phytoplankton and zooplankton taxa. In cases where multiple phytoplankton tows or zooplankton taxa were collected at a given site, the mean isotope value was calculated for that location and used for the isoscapes of "all phytoplankton" or "all zooplankton." Since sampling of two major zooplankton taxonomic groups – euphausiids and amphipods – spanned our entire study area, we generated taxon-specific isoscapes for these taxa, again using mean values for euphausiids or amphipods if multiple replicates were sampled at a given station.

Prior to applying a statistical test, conformance with the test's assumptions was evaluated. Any violations of test assumptions and subsequent data transformations are indicated below. Statistical comparisons of $\delta^{15}N$ and $\delta^{13}C$ values for phytoplankton, all zooplankton taxa, euphausiids, and amphipods of different regions and sampling periods were performed with separate two-way Analyses of Variance (ANOVA) with post-hoc pairwise comparisons. Samples were clustered into five geographic regions: Ross Sea, Amundsen Sea, WAP – all three of the preceding regions are in the ACZ – AZ, and combined PFZ and SAZ (PFZ/SAZ). Model II linear regression analysis was used to examine relationships between zooplankton $\delta^{15}N$ values and surface [NO_3^-]. Since we performed isotopic analysis on homogenized whole organisms, the $\delta^{15}N$ values integrate the oceanographic conditions experienced by the organism over multiple preceding months, not the physical environment at the exact moment and site when the organism was sampled. Thus, we averaged surface [NO_3^-] over a six-month period encompassing the spring and summer, obtaining values of [NO_3^-] from the literature (Table S3), as our samples predominately were collected during the summer. Linear regression analysis was used to assess the relationship between all zooplankton $\delta^{13}C$ values and latitude after log transformation of the data. Similarly, linear regression analysis with square root-transformed data was used to investigate the relationship between all zooplankton $\delta^{13}C$ values and sea surface temperature (SST). As with $\delta^{15}N$ values, the $\delta^{13}C$ values in our study represent an integration of the oceanographic conditions experienced by the zooplankton over several months. Therefore, we used SSTs derived from Gouretski and Koltermann (2004), which used multiple datasets to construct SSTs across the West Antarctic from the Drake Passage to the Ross Sea. All statistical tests were performed in R (R Core Team 2014).

RESULTS

$\delta^{15}N$ Isoscapes

Zooplankton $\delta^{15}N$ values vary significantly across the West Antarctic ($p < 0.001$, ANOVA), and sampling period has no significant effect on the observed gradient. Ross Sea and Amundsen Sea zooplankton have significantly higher $\delta^{15}N$ values (6.2 ± 0.8 ‰ and 6.2 ± 0.6 ‰, respectively; $n = 7$ for both regions; mean ± standard deviation) than those from the WAP (4.1 ± 0.7 ‰, $n = 10$), AZ (3.7 ± 0.6 ‰, $n = 5$), and PFZ/SAZ (3.3 ± 0.6 ‰, $n = 5$) (Figs. 2a and S1, Table S1, $p < 0.001$ for all Bonferroni post-hoc pairwise comparisons). Interestingly, these isotope gradients are not reflected in the phytoplankton $\delta^{15}N$ values across this region, which do not vary significantly across region but do vary significantly among sampling periods ($p = 0.004$, ANOVA, Fig. S2a, Table S4).

The $\delta^{15}N$ isoscapes for euphausiids and amphipods are similar to the composite isoscape of all zooplankton. The $\delta^{15}N$ values of euphausiids vary significantly among the regions ($p <$ 0.001, ANOVA), with euphausiid $\delta^{15}N$ values significantly higher in the Ross Sea (6.5 ± 0.4 ‰, n = 6) and Amundsen Sea (6.7 ± 0.9 ‰, n = 6) than in the WAP (4.1 ± 0.8 ‰, n = 10), AZ (4.8 ± 0.9 ‰, n = 5), and PFZ/SAZ (3.8 ± 1.0 ‰, n = 5) based on Bonferroni post-hoc tests ($p < 0.001$ in all cases, except p = 0.02 and 0.004 for the Ross Sea versus AZ and Amundsen Sea versus AZ, correspondingly, Fig. 3a). Although sample sizes are low, the $\delta^{15}N$ pattern of amphipods across the five regions (Fig. 4a) is similar to that of all zooplankton: the $\delta^{15}N$ values of amphipods in the Ross (6.9 ± 0.8 ‰, n = 3) and Amundsen (6.2 ± 1.2 ‰, n = 3) Seas are higher than those in the WAP (3.8 ± 2.7 ‰, n = 2), the AZ (3.4 ± 1.2 ‰, n = 4), and the PFZ/SAZ (3.4 ± 1.4 ‰, n = 4). Spatial coverage is poor for the other taxa, but the $\delta^{15}N$ patterns for pteropods, salps, copepods, and mixed plankton (0-200 µm, 4% formaldehyde-seawater mixture) are consistent with the significant patterns of all zooplankton taxa and euphausiids (Figs. S3a, S4a, S5a, and S6a, Tables S1 and S2). The $\delta^{15}N$ values of zooplankton are inversely related to the surface [NO_3^-] (p = 0.05, R^2 = 0.8, Fig. S7).

δ^{13}C Isoscapes

The $\delta^{13}C$ values for all zooplankton taxa vary significantly across the West Antarctic ($p <$ 0.001, ANOVA) and sampling period does not significantly affect these patterns (Figs. 2b and S1, Table S1). Zooplankton from the Ross Sea have significantly lower $\delta^{13}C$ values (-27.5 ± 1.6 ‰, n = 7) than those from the WAP (-25.1 ± 1.7 ‰, n = 10) and the PFZ/SAZ (-24.2 ± 0.9 ‰, n = 5) (Bonferroni post-hoc test p-values of 0.01 and 0.002, respectively). Additionally, all zooplankton $\delta^{13}C$ values from AZ waters (-27.1 ± 0.7 ‰, n = 5) are significantly lower than those of the PFZ/SAZ (p = 0.01 in Bonferroni post-hoc test). All zooplankton from the

Amundsen Sea have $\delta^{13}C$ values (-26.1 ± 1.1 ‰, *n* = 7) alike those from the Ross Sea. Similar to the $\delta^{15}N$ patterns, phytoplankton $\delta^{13}C$ values are not significantly different among these regions in contrast with the zooplankton $\delta^{13}C$ pattern (Fig. S2b). Additionally, phytoplankton $\delta^{13}C$ values do not vary significantly among sampling time periods (Table S4).

The $\delta^{13}C$ isoscapes for euphausiids and amphipods follow the same pattern as the composite $\delta^{13}C$ isoscape of all zooplankton. Euphausiid $\delta^{13}C$ values are -26.9 ± 1.0 ‰ (*n* = 6) for the Ross Sea, -25.9 ± 1.3 ‰ (*n* = 6) for the Amundsen Sea, -25.3 ± 1.7 ‰ (*n* = 10) for the WAP, -26.9 ± 0.5 ‰ (*n* = 5) for the AZ, and -24.1 ± 0.8 ‰ (*n* = 5) for the PFZ/SAZ (Fig. 3b). Ross Sea and AZ euphausiids have significantly lower $\delta^{13}C$ values than those from the PFZ/SAZ ($p = 0.01$ and 0.02, respectively, in Bonferroni post-hoc tests). Amphipod $\delta^{13}C$ values are -26.5 ± 2.3 ‰ (*n* = 3), -26.0 ± 1.7 ‰ (*n* = 3), -25.7 ± 0.2 ‰ (*n* = 2), -27.2 ± 0.7 ‰ (*n* = 4), and -24.4 ± 1.5 ‰ (*n* = 4) for the Ross Sea, Amundsen Sea, WAP, AZ, and PFZ/SAZ, respectively, and there are no significant differences among the five regions (Fig. 4b). Again, the smaller sample sizes of amphipods relative to those of all zooplankton and euphausiids may explain the lack of significant spatial variability. Consistent with the pattern observed for all zooplankton taxa, $\delta^{13}C$ values of both euphausiids and amphipods increase with decreasing latitude: Ross Sea < Amundsen Sea < WAP < PFZ/SAZ, and $\delta^{13}C$ values for the AZ are lower than PFZ/SAZ and alike those of the ACZ regions. The $\delta^{13}C$ patterns of the other taxa – pteropods, salps, copepods, and mixed plankton (0-200 µm, 4% formaldehyde-seawater mixture) – are similar to the significant patterns observed in all zooplankton taxa and euphausiids (Figs. S3b, S4b, S5b, and S6b, Table S1 and S2). Zooplankton $\delta^{13}C$ values significantly decrease with increasing latitude ($p = 0.03$ and $R^2 = 0.1$, Fig. S8) and decreasing SST ($p = 0.04$ and $R^2 = 0.1$ from a linear regression analysis, Fig. S9).

DISCUSSION

Understanding spatial and temporal variations in isotopic baselines is critical to successful application of ecogeochemical approaches to questions of food web architecture, biogeochemical cycling, and animal movement in dynamic marine environments, like the Southern Ocean (Graham et al. 2010, McMahon et al. 2013a). We find strong gradients in both nitrogen and carbon stable isotope values of zooplankton across the five distinct biogeographic zones of the West Antarctic (Fig. 2). These geospatial patterns appear to be driven by regional gradients in biogeochemistry, productivity, and oceanography. Interestingly, we find no such coherent geospatial gradients in phytoplankton isotope values (Fig. S2). This lack of parallel gradients is likely a function of the short turnover times and fast integration rates (days to weeks) of phytoplankton in this highly dynamic system compared to the longer integration signal from zooplankton (months). Phytoplankton communities are highly dynamic, experiencing considerable variability in species composition, biomass, growth rate and so on, over relatively short scales of time and space (Cloern & Jassby 2010, Zingone et al. 2010). As such, the phytoplankton isotope values represent snapshots of local isotopic baseline signals and the spatial gradients do not become apparent until the local signals are integrated over longer time periods in the higher trophic level zooplankton (Mullin et al. 1984, Pinkerton et al. 2013). For this reason, we focus on zooplankton for the remainder of this discussion of West Antarctic isoscapes.

δ^{15}N Isoscapes Track Productivity Gradients

We observe a strong spatial gradient in zooplankton isotope values from low δ^{15}N values in the WAP, AZ, and PFZ/SAZ to high values in the Ross and Amundsen Seas. The δ^{15}N values of all zooplankton from the Ross and Amundsen Seas are about 2 ‰ higher than those from the WAP and 3 ‰ higher than those from the PFZ/SAZ (Fig. 2a). These patterns in zooplankton $\delta^{15}N$ values are consistent with previously reported data for the region. Pinkerton et al. (2013) report mean (± standard deviation) lipid-extracted zooplankton $\delta^{15}N$ values of 6.1 ± 2.3 ‰ across 14 zooplankton taxa from the Ross Sea (austral summer 2008), indistinguishable from the mean for our Ross Sea zooplankton samples (6.2 ± 0.8 ‰), despite the fact that our samples had been collected in both the austral summers of 2007/08 (n = 1) and 2010/11 (n = 6). Similarly, Schmidt et al. (2003) report mean (± standard deviation) $\delta^{15}N$ values for zooplankton (without lipid extraction) collected from the PFZ/SAZ and 65 °S (similar latitude to that of the WAP) of 3.6 ± 1.1 ‰ (all 15 taxa) and 3.5 ± 1.1 ‰ (all 4 taxa), respectively, between 1996 and 2000 that are similar to our $\delta^{15}N$ values for all zooplankton from the PFZ/SAZ (3.3 ± 0.6 ‰) and the WAP (4.1 ± 0.7 ‰) which had been obtained in the early fall of 2015 and the austral summers of 2007/08 and 2010/11, correspondingly. McMahon et al. (2013b) use meta-analyses of published $\delta^{15}N$ values to produce a global $\delta^{15}N$ isoscape. Although much of the West Antarctic is not included in the isoscape due to a paucity of data, their analysis suggests $\delta^{15}N$ values for the WAP of ~ 3 ‰, similar to our measurements, but higher values for the AZ, PFZ, and SAZ (e.g., of 4-6 ‰) than we observe. However, little data are available for these three regions and, thus their isotopic values are largely driven by data for the WAP and South American coast.

The observed patterns in $\delta^{15}N$ variation within the West Antarctic isoscape likely reflect variable NO_3^- drawdown associated with gradients in productivity (Wada et al. 1987, Altabet & Francois 1994, Waser et al. 2000). The Southern Ocean is the largest high nutrient, low chlorophyll (HNLC) region in the world, with the majority of NO_3^- in the surface waters remaining unused on an annual basis due to iron limitation. As a result, surface [NO_3^-] is relatively high and phytoplankton and zooplankton $\delta^{15}N$ values are relatively low (de Baar et al. 1990, Martin et al. 1990, Altabet & Francois 2001). However, localized regions of more complete NO_3^- utilization associated with high rates of primary productivity may result in increased $\delta^{15}N$ values of phytoplankton and, consequently, zooplankton (DiFiore et al. 2009).

Our $\delta^{15}N$ spatial pattern suggests lower nutrient utilization and productivity in the pelagic PFZ/SAZ and off the WAP (where the continental shelf is narrow) than on the large continental margins of the Amundsen and Ross Seas, which is consistent with the results of prior studies on West Antarctic productivity. The Ross Sea – where the large Ross Sea and Terra Nova Bay polynyas form each spring – exhibits high annually integrated productivity (~ 503 Tg C a^{-1}) on an annual basis compared to other Southern Ocean sectors (Arrigo et al. 1998, 2008, Smith & Comiso 2008). Smith and Cosimo (2008) report that productivity decreased from the southern Ross Sea (2.74 g C m^{-2} d^{-1}) to the central Ross Sea (2.26 g C m^{-2} d^{-1}) to the WAP (1.56 g C m^{-2} d^{-1}). More recently, the Amundsen Sea has been shown to experience high productivity due to iron inputs and stratification from melting glaciers, with water column productivity ranging from 1.56 (sea ice) to 4.18 (Pine Island polynya) g C m^{-2} d^{-1} (Alderkamp et al. 2012). We hypothesize that the high productivity and NO_3^- drawdown in extensive coastal polynyas of the Ross and Amundsen Seas, resulting from glacial inputs of iron, enhanced light availability, and water column stratification (Gordon et al. 2000, Arrigo et al. 2015), lead to higher $\delta^{15}N_{baseline}$ values compared to the WAP and HNLC zones beyond the continental margin.

Our hypothesis that productivity gradients drive the strong gradient in zooplankton $\delta^{15}N$ values is also supported by work in other sectors of the Southern Ocean. DiFiore et al. (2009) measured the $\delta^{15}N$ value of suspended particulate organic nitrogen (PN) along the East Antarctic continental margin, including Dumont the D'Urville Sea, Davis Sea, and Prydz Bay. They document a shift in PN $\delta^{15}N$ values from < 1.5 ‰ for samples from more offshore, pelagic locations to values of ~ 5 ‰ in persistent coastal polynyas, productivity "hot spots" where NO_3^- drawdown is extensive (DiFiore et al. 2009). Similarly, Schmidt et al. (2003) report $\delta^{15}N$ values of POM, *Euphausia superba* furcilia larvae, and copepods (*Metridia gerlachei* and *Calanoides acutus*) that are 4 to 5 ‰ higher in Marguerite Bay (67°30' S, 70° W), in the WAP region, than in the Lazarev Sea (~ 69° S, 5° W), likely due to differing degrees of NO_3^- utilization by phytoplankton between these two sites. During their time of sample collection, phytoplankton abundance in the Lazarev Sea was low (~ 0.5 µg chlorophyll *a* L^{-1}) in contrast with Marguerite Bay, which was experiencing a several-month-long diatom bloom (7-10 µg chlorophyll *a* L^{-1}) (Schmidt et al. 2003). Indeed, visualizations of surface [NO_3^-] in the WAP during the austral summer reveal pockets of low [NO_3^-] (e.g., [NO_3^-] of ~ 7 µmol L^{-1}), likely due to phytoplankton NO_3^- consumption, largely along the coast within bays and fjords, while much of the WAP region has surface [NO_3^-] of 20 to 27 µmol L^{-1} (Fig. 5).

In contrast to our observations, previous modeling work by Somes et al. (2010) predict relatively consistent $\delta^{15}N_{baseline}$ values across the West Antarctic, and Jaeger et al. (2010a) model a decrease in $\delta^{15}N_{baseline}$ values from the STZ towards the AZ. Both the Somes et al. (2010) and Jaeger et al. (2010a) isoscapes focus on oceanic regions, beyond the continental margin, where the NO_3^- pool remains large and underutilized due to apparent iron limitation (Boyd et al. 2012). As such, productivity and associated NO_3^- drawdown, and thus $\delta^{15}N$ values of POM, decrease from the more productive STZ into the HNLC oceanic area of the Southern Ocean. Our isoscapes include continental margins across the West Antarctic, which are likely to experience higher productivity than oceanic regions due to increased iron inputs and stratification from glacial melting. The WAP has a relatively narrow continental shelf with reduced productivity compared to the wide shelves of the Ross and Amundsen Seas. Thus, our $\delta^{15}N_{baseline}$ values increase from the HNLC oceanic area to the continental margins, and this gradient is pronounced in the Amundsen and Ross Sea sectors since they have extensive continental shelves. Additionally, our linear regression analysis reveals increasing zooplankton $\delta^{15}N$ values with decreasing surface [NO_3^-] in West Antarctica, indicating that high coastal productivity drives low surface [NO_3^-] and, consequently, high $\delta^{15}N_{baseline}$ values.

The productivity gradient within our systems offers the most parsimonious explanation for the observed $\delta^{15}N$ isoscape along the continental shelf of the West Antarctic. However, it is possible that either variability in the zooplankton taxa obtained from each region or spatially shifting trophic positions for sampled taxa contribute to the observed nitrogen isoscape patterns. Changes in zooplankton sampling are an unlikely source of the observed pattern because even when analyzed at the level of individual taxon, zooplankton $\delta^{15}N$ values in the Amundsen and Ross Seas are ~ 2 ‰ higher than those in the WAP (Figs. 3a, 4a, S3a, S4a, S5a, and S6a). While we cannot rule out potential variations in zooplankton trophic position as a contributor to the spatial pattern in $\delta^{15}N_{baseline}$ values, it should be noted that the observed $\delta^{15}N$ gradient would imply nearly a full trophic level change although the $\delta^{15}N$ gradient is present in the dominantly herbivorous *E. superba* (Siegel & Loeb 1995, Nicol 2006, Pinkerton et al. 2010). Additionally, perhaps spatial variation in the utilization of different nutrient sources (i.e., nitrate and ammonium) by phytoplankton may contribute to our observed $\delta^{15}N$ gradient (Graham et al. 2010). These possible factors should be explored in future research..

Importantly, the physical conditions affecting primary productivity and nutrient drawdown in West Antarctica vary seasonally and inter-annually as a result of regional and global climate events (Wainwright & Fry 1994, Smith et al. 1998, Kwok & Comiso 2002, Arrigo

& van Dijken 2004, Arrigo et al. 2008). These temporal dynamics can have a strong impact on the geospatial isotope patterns in this region, depending on organism integration time. For instance, productivity slowly increases in the early austral spring (October) as a result of increased insolation and iron inputs from retreating sea ice (Arrigo & van Dijken 2003), reaching peak bloom in the austral summer, before returning to pre-bloom levels by March or April (Arrigo & van Dijken 2003). The temporal progression of phytoplankton blooms results in a corresponding seasonal pattern of nutrient drawdown and $\delta^{15}N_{baseline}$ value shift, whereby the surface layer [NO_3^-] is low and the $\delta^{15}N_{baseline}$ value is high at the bloom peak (DiFiore et al. 2006, DiFiore et al. 2009). Most of our zooplankton samples were collected during the austral summer, largely between mid-December and late-January. Some of our zooplankton samples were obtained during the early austral fall. Sampling period did not significantly affect a region's $\delta^{15}N$ value for our all zooplankton, euphausiid, or amphipod isoscapes. Yet, since our zooplankton sampling was predominately within the summer, integrating oceanographic conditions over multiple preceding months, our isoscapes may not fully capture the full seasonal variation in productivity and, consequently, $\delta^{15}N_{baseline}$ values. Selection of an isoscape with appropriate time integration for the temporal scale of a research question is important and our isoscape best represents geospatial gradients in West Antarctica occurring over a period of months and, perhaps, years, not short time scales of weeks or days.

On longer time scales, the dominant climate modes in the Southern Hemisphere, resulting in interannual variation in environmental conditions, are the Southern Annular Mode (SAM) and the El Niño-Southern Oscillation (ENSO) (Arrigo et al. 2008, Stammerjohn et al. 2008), which result in a whole host of interannual variations in environmental conditions (e.g., Smith et al. 1999, Croxall et al. 2002). SAM and ENSO co-vary; La Niña (El Niño) is associated with positive (negative) SAM. La Niña and positive SAM events are associated with colder conditions and more sea ice in the Ross and Amundsen Seas, while the WAP experiences warmer conditions and less sea ice (Arrigo et al. 2008, Stammerjohn et al. 2008). The opposite scenario has been observed for El Niño and negative SAM events (Arrigo et al. 2008, Stammerjohn et al. 2008).

Visualizations of surface [NO_3^-] off the WAP during times of varying ENSO conditions in recent years for which data is available (Ducklow et al. 2017a,b) show possible effects of ENSO events on surface [NO_3^-] in this region (Figs. 5, S10, and S11). Areas of high NO_3^- drawdown near the WAP coast take place during austral summers with or without a strong ENSO event (Figs. 5, S10, and S11). However, the extent of nearshore NO_3^- drawdown appears low, intermediate, and high during a La Niña event, no strong ENSO event, and an El Niño event, respectively, with presumably opposite (but unmeasured) effects in the Amundsen and Ross Seas. The surface [NO_3^-] minima along the WAP coast are approximately twelve, seven, and four μmol L^{-1} during periods with a La Niña event, no strong ENSO event, and an El Niño event, respectively (Figs. 5, S10, and S11).

Our comparison of $\delta^{15}N_{baseline}$ values among different West Antarctic regions uses data from zooplankton samples collected during times of La Niña events (periods of December 2007 through January 2008 and December 2010 through January 2011) or an El Niño (early fall 2015) event. While differing ENSO conditions across sampling periods may contribute to some of the observed variation in $\delta^{15}N_{baseline}$ values within this isoscape, it should be noted that sampling period did not have a significant effect on zooplankton $\delta^{15}N$ values. For the WAP, a region sampled during different ENSO conditions, $\delta^{15}N_{baseline}$ values of zooplankton collected during strong La Niña events (December 2010 through January 2011 or December 2007 through

January 2008) are similar to those collected during a weak-to-moderate El Niño event (early fall 2015). Our findings suggest that the observed nitrogen isotope gradients in the West Antarctic are robust at least over the sampling period of this study. However, future research should further examine the extent of $\delta^{15}N_{baseline}$ value variation in West Antarctica resulting from the climate modes over longer time scales.

δ^{13}C isoscapes track temperature gradients

Our carbon isoscape reveals an inverse relationship between $\delta^{13}C_{baseline}$ values and latitude. The Ross Sea (sampling stations at latitudes between 71 °S and 79 °S) has significantly lower δ^{13}C values than the WAP and PFZ/SAZ (sampling latitudes between 69 °S and 55 °S) by about 2 ‰ and 3 ‰, respectively (Fig. 2b). These patterns in zooplankton δ^{13}C value are generally consistent with previously reported data for the region. Pinkerton et al. (2013) report Ross Sea zooplankton have a mean δ^{13}C value of -26.7 ± 2.0 ‰ (14 taxa) for Ross Sea zooplankton, which is similar to that for the composite of all Ross Sea zooplankton in our study (-27.5 ± 1.6 ‰). Schmidt et al. (2003) report a comparable pattern of decreasing zooplankton δ^{13}C values from the PFZ/SAZ (-25.6 ± 3.3 ‰; 15 taxa) to 65 °S (-30.0 ± 0.6 ‰; 4 taxa) as we do across a similar latitudinal gradient, though their absolute values are lower than ours. Schmidt et al. (2003) did not lipid extract their samples, which may explain the lower δ^{13}C values they report. Lastly, McMahon et al. (2013b) produced a global δ^{13}C isoscape from meta-analyses of published plankton δ^{13}C values. While their global isoscape had limited sample coverage for the area of interest in our study (e.g., no coverage in the Amundsen Sea and only part of the Ross Sea) they found a decrease in plankton $\delta^{13}C_{baseline}$ values from -23 to -25 ‰ in the PFZ/SAZ to values between -25 and -30 ‰ in the AZ/WAP, similar to the δ^{13}C spatial gradient in our study

The observed inverse relationship between $\delta^{13}C$ variation and latitude within the West Antarctic isoscape is likely explained by the latitudinal gradient in SST (Cherel & Hobson 2007, Quillfeldt et al. 2010, Quillfeldt et al. 2015). This is because the $\delta^{13}C$ value of primary production is greatly influenced by the CO_2 solubility in the ocean, which increases with decreasing temperature, as the fractionation associated with photosynthetic uptake of CO_2 is strongly expressed in high [$CO_{2(aq)}$] environments (Goericke & Fry 1994, Graham et al. 2010). Using SST values for our sampling locations (Gouretski & Koltermann 2004) within these regions (-1.3 °C, 0.1 °C, and 4 °C for the Ross Sea, WAP, and PFZ/SAZ, correspondingly) and equations derived by Rau et al. (1989) relating SST, CO_2 (aq), and phytoplankton $\delta^{13}C$ values, we correctly predict an offset between Ross Sea and PFZ/SAZ zooplankton $\delta^{13}C$ values of 3 ‰ and an offset of 1 ‰ between the Ross Sea and WAP zooplankton $\delta^{13}C$ values. Thus, SST may completely explain the difference in zooplankton $\delta^{13}C$ values between the Ross Sea and PFZ/SAZ. However, our calculated offset between zooplankton $\delta^{13}C$ values from the Ross Sea and WAP is less than our measured offset, suggesting other drivers besides just SST may be influencing this gradient in $\delta^{13}C_{baseline}$ values.

Although many studies have indicated SST and, in association CO_2 solubility, drives variation in phytoplankton $\delta^{13}C$ values (Rau et al. 1989, Rau et al. 1991, Cherel & Hobson 2007, Quillfeldt et al. 2010, Quillfeldt et al., 2015), a number of other potential factors, including dissolved inorganic carbon (DIC) source, growth and photosynthetic rates, and phytoplankton size and geometry, can influence phytoplankton, and thus zooplanton, $\delta^{13}C$ values (Descolas-Gross and Fontugne 1985, Falkowski 1991, Popp et al. 1998, Popp et al. 1999, Villinksi et al. 2001, Kennedy et al. 2002, Papadimitriou et al. 2009, Kohlbach et al. 2016). Variation in $\delta^{13}C_{DIC}$ values is likely not a substantial factor shaping $\delta^{13}C_{baseline}$ values in West Antarctica because prior research has found areas of the Southern Ocean, such as the Drake Passage, exhibit considerable gradients in phytoplankton $\delta^{13}C$ values with little change to source DIC values (Rau et al. 1991). However, future work will be needed to determine whether the local regions of plankton $\delta^{13}C$ offsets are explained by local gradients in cell size or geometry, growth rate, or CO_2 drawdown not directly related to SST.

As was the case with nitrogen, temporal variation in carbon isotope gradients is an important factor to consider when evaluating isoscape structure. SSTs fluctuate seasonally with sea ice conditions, as well as interannually with variation in climate modes (Wainwright & Fry 1994, Kwok & Comiso 2002, Arrigo et al. 2008). As described above, La Niña and positive SAM events are associated with colder conditions and more sea ice in the Ross and Amundsen Seas, while the WAP experiences warmer conditions and less sea ice (Arrigo et al. 2008, Stammerjohn et al. 2008). El Niño and negative SAM events experience the reverse situation (Arrigo et al. 2008, Stammerjohn et al. 2008). Prior work has suggested that these climate modes may cause SST anomalies of up to ± 0.5 °C (Yuan 2004). This temporal variation is less than the SST range spanning our study region, suggesting that the temporal variability will not overpower the spatial gradient signal. For instance, our $\delta^{13}C$ isoscapes for all zooplankton, euphausiids, amphipods, and phytoplankton are not significantly affected by sampling period. However, our sampling was limited primarily to the austral summer and did not cover several years. Thus, our $\delta^{13}C_{baseline}$ may not fully capture the true dynamism of seasonal and interannual patterns, which should be explored more thoroughly in future studies.

CONCLUSIONS

This study presents the first empirically derived zooplankton isoscapes for West Antarctica, reflecting dynamic biogeochemical change across the region. Our isoscapes reveal an ~ 3 ‰ increase in $\delta^{15}N$ values from HNLC oceanic regions to the continental margins of West Antarctica, which we attribute to increasing productivity and nutrient utilization. Conversely, there is an ~ 3 ‰ decrease in $\delta^{13}C$ values from the PFZ/SAZ to the Ross Sea, which we attribute primarily to decreasing SST. These isoscapes provide a critical first look at the strong geospatial gradients in stable carbon and nitrogen isotope values across major biogeographic zones of the West Antarctic. Such isoscapes will open new doors for ecological, paleoecological, and oceanographic studies of food web architecture, biogeochemical cycling, and animal migration in the Southern Ocean. Furthermore, these isoscapes will serve as a benchmark for future studies of biogeochemical change in this highly dynamic system, which is experiencing some of the most rapid climate change on Earth.

It is important to recognize the limitations of our $\delta^{15}N$ and $\delta^{13}C$ isoscapes, which apply to all static isoscape approaches. Our isoscapes were generated from a limited number of opportunistically collected samples, requiring interpolation among data points to generate the smooth gradient contours. The resulting geospatial patterns are strong and consistent across a number of independent taxa, but additional sampling will improve the accuracy and precision of the isoscapes. Our hope is that our isoscapes will encourage more empirical sampling to enhance the evaluation of the geospatial isotope patterns in this critical region and better understand the underlying mechanisms driving those patterns. In addition, our isoscape represents a limited period of time. Temporal variability in regional oceanography (e.g., SST), sources of N or C fueling primary production, phytoplankton growth rate, community composition, and so on can all impact the geospatial distribution of stable isotope values in space and time. In particular, further studies on the role of climate modes (e.g., ENSO) on interannual variation in baseline isotope values will allow for improved construction and application of isoscapes. Future work should advance Southern Ocean isoscapes to better capture temporal variation in baseline isotope values and increase spatial resolution.

ACKNOWLEDGEMENTS

We thank Deborah Steinberg, Kate Ruck, Heidi Geisz, and Rebecca Dickhut for providing us with an array of samples. We are grateful to Colin Carney and Dyke Andreasen for laboratory assistance. We also thank the crew and staff on the *RV Oden* (austral summers of 2007/08 and 2010/11), *RV Nathaniel B. Palmer* (austral summer 2011/12), and *SV Lawrence M. Gould* (early fall 2015), as well as the staff of the PAL-LTER (from 2007 through 2011). This project was supported by the National Science Foundation (NSF ANT-1142108 and OPP-1347911). We are grateful to the anonymous reviewers and editor for their valuable guidance in improving this manuscript.

FIGURES

Figure 1. Zooplankton sampling locations for developing $\delta^{15}N$ and $\delta^{13}C$ isoscapes across five Southern Ocean biogeographic zones.

Figure 2. $\delta^{15}N$ (a) and $\delta^{13}C$ (b) values (‰) of all zooplankton taxa from West Antarctica.

Figure 3. $\delta^{15}N$ (a) and $\delta^{13}C$ (b) values (‰) of all euphausiids from West Antarctica.

Figure 4. $\delta^{15}N$ (a) and $\delta^{13}C$ (b) values (‰) of all amphipods from West Antarctica.

Figure 5. Surface nitrate concentrations (μmol L^{-1}) off the WAP for the austral summer (January and February) of 2006, a time without a strong ENSO event.

SUPPLEMENTAL MATERIAL

Figure S1. $\delta^{15}N$ versus $\delta^{13}C$ values (‰) of zooplankton from West Antarctica.

Figure S2. $\delta^{15}N$ (a) and $\delta^{13}C$ (b) values (‰) of phytoplankton from West Antarctica.

Figure S3. $\delta^{15}N$ (a) and $\delta^{13}C$ (b) values (‰) of pteropods from West Antarctica.

Figure S4. $\delta^{15}N$ (a) and $\delta^{13}C$ (b) values (‰) of salps from West Antarctica.

Figure S5. $\delta^{15}N$ (a) and $\delta^{13}C$ (b) values (‰) of copepods from West Antarctica.

Figure S6. $\delta^{15}N$ (a) and $\delta^{13}C$ (b) values (‰) of Ross Sea mixed, formalin-exposed plankton (0-200 μm).

Figure S7. Mean $\delta^{15}N$ values (‰) of all zooplankton taxa versus mean nitrate concentration (μmol L^{-1}) for each of our five geographic regions.

Figure S8. $\delta^{13}C$ values (‰) of all zooplankton taxa versus latitude of sampling location.

Figure S9. $\delta^{13}C$ values (‰) of all zooplankton taxa versus sea surface temperature (°C) of sampling location.

Figure S10. Surface nitrate concentrations (μmol L^{-1}) off the WAP for austral summer (January and February) of 2007, which experienced El Niño conditions.

Figure S11. Surface nitrate concentrations (μmol L^{-1}) off the WAP for austral summer (January and February) of 2008, which experienced strong La Niña conditions.

Table S1. Isotopic data for all zooplankton.

Table S2. Isotopic values of formalin-exposed plankton (0-200 μm) from the Ross Sea.

Table S3. Surface nitrate concentrations (μmol L^{-1}) determined for West Antarctic regions.

Table S4. Isotopic values of phytoplankton.

LITERATURE CITED

Alderkamp AC, Mills MM, van Dijken GL, Laan P, Thuróczy CE, Gerringa LJA, de Baar HJW, Payne CD, Visser RJW, Buma AGJ, Arrigo KR (2012) Iron from melting glaciers fuels phytoplankton blooms in the Amundsen Sea (Southern Ocean): Phytoplankton characteristics and productivity. Deep Sea Res II 71-76:32-48

Altabet MA, Francois R (1994) Sedimentary nitrogen isotopic ratio as a recorder for surface ocean nitrate utilization. Global Biogeochem Cycles 8:103-116

Altabet MA, Francois R (2001) Nitrogen isotope biogeochemistry of the Antarctic Polar Frontal Zone at 170 W. Deep Sea Res Part II 48:4247-4273

Arrigo KR, Weiss AM, Smith WO (1998) Physical forcing of phytoplankton dynamics in the southwestern Ross Sea. J Geophys Res, C, Oceans 103:1007-1021

Arrigo KR, DiTullio GR, Dunbar RB, Robinson DH, VanWoert M, Worthen DL, Lizotte MP (2000) Phytoplankton taxonomic variability in nutrient utilization and primary production in the Ross Sea. J Geophys Res, C, Oceans 105:8827-8846

Arrigo KR, van Dijken GL (2003) Phytoplankton dynamics within 37 Antarctic coastal polynya systems. J Geophys Res, C, Oceans 108:3271

Arrigo KR, van Dijken GL (2004) Annual changes in sea-ice, chlorophyll a, and primary production in the Ross Sea, Antarctica. Deep Sea Res II 51:117-138

Arrigo KR, van Dijken GL, Bushinsky S (2008) Primary production in the Southern Ocean, 1997–2006. J Geophys Res, C, Oceans 113:C08004

Arrigo KR, van Dijken GL, Strong AL (2015) Environmental controls of marine productivity hot spots around Antarctica. J Geophys Res, C, Oceans, 120:5545-5565

Atkinson A, Siegel V, Pakhomov E, Rothery P (2004) Long-term decline in krill stock and increase in salps within the southern ocean. Nature 432:100-103

Barth A, Alvera A, Troupin C, Ouberdous M, Beckers JM (2010) A web interface for griding arbitrarily distributed in situ data based on Data-Interpolating Variational Analysis (DIVA). Adv Geosci 28:29-37

Bidigare RR, Fluegge A, Freeman KH, Hanson KL, Hayes JM, Hollander D, Jasper JP, King LL, Laws EA, Milder J, Millero FJ, Pancost R, Popp BN, Steinberg PA, Wakeham SG (1997) Consistent fractionation of ^{13}C in nature and in the laboratory: Growth-rate effects in some haptophyte algae. Global Biogeochem Cycles 11:279-292

Bligh EG, Dyer WJ (1959) A rapid method of total lipid extraction and purification. Can J Biochem Physiol 37:911-917

Boecklen, W.J., Yarnes, C.T., Cook, B.A. and James, A.C., 2011. On the use of stable isotopes in trophic ecology. Annu Rev Ecol Evol Syst 42:411-440

Bowen GJ (2010) Isoscapes: spatial pattern in isotopic biogeochemistry. Annu Rev Earth Planet Sci 38:161-187

Boyd PW, Arrigo KR, Strzepek R, Dijken GL (2012) Mapping phytoplankton iron utilization: Insights into Southern Ocean supply mechanisms. J Geophys Res, C, Oceans 117:C06009

Brault EK (2012) Evaluating Persistent Organic Pollutants (POPs) and Mercury in the West Antarctic Peninsula (WAP) Food Web, with a Focus on Antarctic Fur Seals (*Arctocephalus gazella*). MS thesis, Virginia Institute of Marine Sciences, Gloucester Point, VA.

Cherel Y, Hobson KA (2007) Geographical variation in carbon stable isotope signatures of marine predators: a tool to investigate their foraging areas in the Southern Ocean. Mar Ecol Prog Ser 329:281-287

Chikaraishi Y, Ogawa NO, Kashiyama Y, Takano Y, Suga H, Tomitani A, Miyashita H, Kitazato H, Ohkouchi N (2009) Determination of aquatic food-web structure based on compound-specific nitrogen isotopic composition of amino acids. Limnol Oceanogr Methods 7:740-750

Cloern, JE, Jassby AD (2010) Patterns and scales of phytoplankton variability in estuarine–coastal ecosystems. Estuar Coasts 33:230-241

Croxall JP, Trathan PN, Murphy EJ (2002). Environmental change and Antarctic seabird populations. Science 297:1510-1514

Croxall JP, Nicol S (2004) Management of Southern Ocean fisheries: global forces and future sustainability. Antarct Sci 16:569-584

de Baar HJ, Buma AG, Nolting RF, Cadée GC, Jacques G, Tréguer PJ (1990) On iron limitation of the Southern Ocean: experimental observations in the Weddell and Scotia Seas. Mar Ecol Prog Ser 65:105-122

Descolas-Gros C, Fontugne MR (1985) Carbon fixation in marine phytoplankton: carboxylase activities and stable carbon-isotope ratios; physiological and paleoclimatological aspects. Mar Biol 87:1-6

DiFiore PJ, Sigman DM, Trull TW, Lourey MJ, Karsh K, Cane G, Ho R (2006) Nitrogen isotope constraints on subantarctic biogeochemistry. J Geophys Res, C, Oceans 111:C08016

DiFiore PJ, Sigman DM, Dunbar RB (2009) Upper ocean nitrogen fluxes in the Polar Antarctic Zone: Constraints from the nitrogen and oxygen isotopes of nitrate. Geochem Geophys Geosyst 10:Q11016

Dobush GR, Ankney CD, Krementz DG (1985) The effect of apparatus, extraction time, and solvent type on lipid extractions of snow geese. Can J Zool 63:1917-1920

Ducklow, HW, Baker K, Martinson DG, Quetin LB, Ross RM, Smith RC (2007) Marine pelagic ecosystems: The West Antarctic Peninsula. Philos Trans R Soc Lond B Biol Sci 362:67-94

Ducklow HW, Clarke A, Dickhut R, Doney SC, Geisz H, Huang K, Martinson DG, Meredith MP, Moeller HV, Montes-Hugo M, Schofield O, Stammerjohn SE, Steinberg D, Fraser W (2012) The marine system of the Western Antarctic Peninsula. In: Rogers AD, Johnston NM, Murphy EJ, Clarke A (eds) Antarctic ecosystems: an extreme environment in a changing world, Blackwell Publishing LTD, Hoboken, New Jersey, USA, p 121-159

Ducklow H., M. Vernet, B. Prezelin (2017a) Dissolved inorganic nutrients including 5 macro nutrients: silicate, phosphate, nitrate, nitrite, and ammonium from water column bottle samples collected during annual cruise along western Antarctic Peninsula, 1991-2017. Environmental Data Initiative [http://dx.doi.org/10.6073/pasta/9894dad135256558445e61d1956ff6a6]

Ducklow H., M. Vernet, B. Prezelin (2017b) Dissolved inorganic nutrients including 5 macro nutrients: silicate, phosphate, nitrate, nitrite, and ammonium from water column bottle

samples collected between October and April at Palmer Station, 1991-2016. Environmental Data Initiative [http://dx.doi.org/10.6073/pasta/891c4b10c650e34e32df6fdd927773ba]
Falkowski PG (1991) Species variability in the fractionation of 13C and 12C by marine phytoplankton. J Plankton Res 13:21-28
Falkowski PG, Barber RT, Smetacek V (1998) Biogeochemical controls and feedbacks on ocean primary production. Science 281:200-206
Forcada J, Trathan PN (2009) Penguin responses to climate change in the Southern Ocean. Glob Change Biol 15:1618-1630
Gille ST (2002) Warming of the Southern Ocean since the 1950s. Science 295:1275-1277
Goericke R, Fry B (1994) Variations in marine plankton $\delta^{13}C$ with latitude, temperature, and dissolved CO_2 in the world ocean. Global Biogeochem Cycles 8:85-90
González-Bergonzoni I, Vidal N, Wang B, Ning D, Liu Z, Jeppesen E, Meerhoff M (2015) General validation of formalin-preserved fish samples in food web studies using stable isotopes. Methods Ecol Evol 6:307-314
Gordon LI, Codispoti LA, Jennings JC, Millero FJ, Morrison JM, Sweeney C (2000) Seasonal evolution of hydrographic properties in the Ross Sea, Antarctica, 1996–1997. Deep Sea Res II 47:3095-3117
Gouretski VV, Koltermann KP (2004) WOCE global hydrographic climatology. Berichte des Bundesamtes für Seeschifffahrt und Hydrographie Tech Rep 35:1-52
Graham BS, Koch PL, Newsome SD, McMahon KW, Aurioles D (2010) Using isoscapes to trace the movements and foraging behavior of top predators in oceanic ecosystems. In: West JB, Bowen GJ, Dawson TE, Tu KP (eds) Isoscapes. Springer, Netherlands, p 299-318
Jacobs SS, Giulivi CF, Mele PA (2002) Freshening of the Ross Sea during the late 20th century. Science 297:386-389
Jaeger A, Connan M, Richard P, Cherel Y (2010a) Use of stable isotopes to quantify seasonal changes of trophic niche and levels of population and individual specialization in seabirds. Mar Ecol Prog Ser 401:269-277
Jaeger A, Lecomte VJ, Weimerskirch H, Richard P, Cherel Y (2010b). Seabird satellite tracking validates the use of latitudinal isoscapes to depict predators' foraging areas in the Southern Ocean. Rapid Commun Mass Spectrom 24:3456-3460
Kattner G, Hagen W, Graeve M, Albers C (1998) Exceptional lipids and fatty acids in the pteropod Clione limacina (Gastropoda) from both polar oceans. Mar Chem 61:219-228
Kennedy H, Thomas DN, Kattner G, Haas C, Dieckmann GS (2002) Particulate organic matter in Antarctic summer sea ice: concentration and stable isotopic composition. Mar Ecol Prog Ser 238:1-13
Kohlbach D, Graeve M, A Lange B, David C, Peeken I, Flores H (2016) The importance of ice algae-produced carbon in the central Arctic Ocean ecosystem: Food web relationships revealed by lipid and stable isotope analyses. Limnol Oceanogr 61:2027-2044
Kurle CM, Worthy GA (2002) Stable nitrogen and carbon isotope ratios in multiple tissues of the northern fur seal Callorhinus ursinus: implications for dietary and migratory reconstructions. Mar Ecol Prog Ser 236:289-300
Kwok R, Comiso JC (2002) Southern Ocean climate and sea ice anomalies associated with the Southern Oscillation. J Clim 15:487-501
Lee RF, Hagen W, Kattner G (2006) Lipid storage in marine zooplankton. Mar Ecol Prog Ser 307:273-306

Lorrain A, Graham B, Ménard F, Popp B, Bouillon S, Van Breugel P, Cherel Y (2009) Nitrogen and carbon isotope values of individual amino acids: a tool to study foraging ecology of penguins in the Southern Ocean. Mar Ecol Prog Ser 391:293-306
Marinov I, Gnanadesikan A, Toggweiler JR, Sarmiento JL (2006) The southern ocean biogeochemical divide. Nature 441:964-967
Martin JH, Gordon RM, Fitzwater SE (1990) Iron in Antarctic waters. Nature 345:156-158
MacKenzie KM, Palmer MR, Moore A, Ibbotson AT, Beaumont WR, Poulter DJ, Trueman CN (2011) Locations of marine animals revealed by carbon isotopes. Sci Rep 1:21
MacKenzie KM, Longmore C, Preece C, Lucas CH, Trueman CN (2014) Testing the long-term stability of marine isoscapes in shelf seas using jellyfish tissues. Biogeochemistry 121:441-454
McMahon KW, Hamady LL, Thorrold SR (2013a) A review of ecogeochemistry approaches to estimating movements of marine animals. Limnol Oceanogr 58:697-714
McMahon KW, Hamady L, Thorrold SR (2013b) Ocean ecogeochemistry: a review. Oceanogr Mar Biol Annu Rev 51:327-374
Meredith MP, King JC (2005) Rapid climate change in the ocean west of the Antarctic Peninsula during the second half of the 20th century. Geophys Res Lett 32:L19604
Montes-Hugo M, Doney SC, Ducklow HW, Fraser W, Martinson D, Stammerjohn SE (2009) Recent changes in phytoplankton communities associated with rapid regional climate change along the western western Antarctic Peninsula. Science 323:1470-1473
Montoya JP (2007) Natural abundance of ^{15}N in marine planktonic ecosystems. Stable isotopes in ecology and environmental science. In: Michener R, Laitha K (eds) Stable Isotopes in Ecology and Environmental Science. Blackwell, Malden, MA, p 176-201
Montoya, JP (2008) Nitrogen stable isotopes in marine environments. In: Capone DG, Carpenter EJ, Mulholland MR, Bronk DA (eds) Nitrogen in the marine environment, Academic Press, London, UK, p 1277-1302
Mullin MM, Rau GH, Eppley RW (1984). Stable nitrogen isotopes in zooplankton: some geographic and temporal variations in the North Pacific. Limnol Oceanogr 29:1267-1273
Needoba JA, Waser NA, Harrison PJ, Calvert SE (2003) Nitrogen isotope fractionation in 12 species of marine phytoplankton during growth on nitrate. Mar Ecol Prog Ser 255:81-91
Nicol S (2006) Krill, currents, and sea ice: Euphausia superba and its changing environment. Bioscience 56:111-120
Nicol S, Worby A, Leaper R (2008) Changes in the Antarctic sea ice ecosystem: potential effects on krill and baleen whales. Mar Freshw Res 59:361-382
Orsi AH, Whitworth III T, Nowlin Jr WD (1995) On the meridional extent and fronts of the Antarctic Circumpolar Current Deep Sea Res I 42:641-673
Peterson BJ, Fry B (1987) Stable isotopes in ecosystem studies. Annu Rev Ecol Syst 18:293-320
Pinkerton MH, Bradford-Grieve JM, Hanchet SM (2010) A balanced model of the food web of the Ross Sea, Antarctica. CCAMLR Sci 17:1-31
Pinkerton MH, Forman J, Bury SJ, Brown J, Horn P, O'Driscoll RL (2013) Diet and trophic niche of Antarctic silverfish Pleuragramma antarcticum in the Ross Sea, Antarctica. J Fish Biol 82:141-164
Papadimitriou S, Thomas DN, Kennedy H, Kuosa H, Dieckmann GS (2009) Inorganic carbon removal and isotopic enrichment in Antarctic sea ice gap layers during early austral summer. Mar Ecol Prog Ser 386:15-27

Perkins MJ, McDonald RA, van Veen FJF, Kelly SD, Rees G, Bearhop S (2013) Important impacts of tissue selection and lipid extraction on ecological parameters derived from stable isotope ratios Methods Ecol Evol 4:944-953
Popp BN, Laws EA, Bidigare RR, Dore JE, Hanson KL, Wakeham SG (1998) Effect of phytoplankton cell geometry on carbon isotopic fractionation. Geochim Cosmochim Acta 62:69-77
Popp BN, Trull T, Kenig F, Wakeham SG, Rust TM, Tilbrook B, Griffiths B, Wright SW, Marchant HJ, Bidigare RR, Laws EA (1999) Controls on the carbon isotopic composition of Southern Ocean phytoplankton. Global Biogeochem Cycles 13:827-843Quillfeldt P, Masello JF, McGill RA, Adams M, Furness RW (2010) Moving polewards in winter: a recent change in the migratory strategy of a pelagic seabird? Front Zool 7:1-11
Quillfeldt P, Ekschmitt K, Brickle P, McGill RA, Wolters V, Dehnhard N, Masello JF (2015) Variability of higher trophic level stable isotope data in space and time–a case study in a marine ecosystem. Rapid Commun Mass Spectrom 7:667-674
R Core Team (2014). R: A language and environment for statistical computing. Foundation for Statistical Computing, Vienna, Austria.
Rau GH, Takahashi T, Des Marais DJ (1989) Latitudinal variations in plankton $\delta^{13}C$: implications for CO_2 and productivity in past oceans. Nature 341:516-518
Rau GH, Takahashi T, Des Marais DJ, Sullivan CW (1991) Particulate organic matter δ13C variations across the Drake Passage. J Geophys Res, C, Oceans 96:15131-15135.
Sarakinos HC, Johnson ML, Zanden MJV (2002) A synthesis of tissue-preservation effects on carbon and nitrogen stable isotope signatures. Can J Zool 80:381-387
Schell DM, Barnett BA, Vinette KA (1998). Carbon and nitrogen isotope ratios in zooplankton of the Bering, Chukchi and Beaufort seas. Mar Ecol Prog Ser 162:11-23
Schlitzer R (2015) Ocean Data View (ODV) version (4.7.4). http://odv.awi.de
Schmidt K, Atkinson A, Stübing D, McClelland JW, Montoya J P, Voss M (2003) Trophic relationships among Southern Ocean copepods and krill: some uses and limitations of a stable isotope approach. Limnol Oceanogr 48:277-289
Siegel V, Loeb V (1995) Recruitment of Antarctic krill Euphausia superba and possible causes for its variability. Mar Ecol Prog Ser 123:45-56
Siniff DB, Garrott RA, Rotella JJ, Fraser WR, Ainley DG (2008) Opinion: Projecting the effects of environmental change on Antarctic seals. Antarct Sci 20:425-435
Smith RC, Baker KS, Vernet M (1998) Seasonal and interannual variability of phytoplankton biomass west of the Antarctic Peninsula. J Mar Syst 17:229-243
Smith RC, Ainley D, Baker K, Domack E, Emslie S, Fraser B, Kennett J, Leventer A, Mosley-Thompson E, Stammerjohn S, Vernet M (1999) Marine ecosystem sensitivity to climate change: Historical observations and paleoecological records reveal ecological transitions in the Antarctic Peninsula region. Bioscience 49:393-404
Smith WO, Comiso JC (2008). Influence of sea ice on primary production in the Southern Ocean: A satellite perspective. J Geophys Res, C, Oceans 113:C05S93
Somes CJ, Schmittner A, Galbraith ED, Lehmann MF, Altabet MA, Montoya JP, Letelier RM, Mix AC, Bourbonnais A, Eby M (2010) Simulating the global distribution of nitrogen isotopes in the ocean. Global Biogeochem Cycles 24:GB4019
Stammerjohn SE, Martinson DG, Smith RC, Yuan X, Rind D (2008) Trends in Antarctic annual sea ice retreat and advance and their relation to El Niño–Southern Oscillation and Southern Annular Mode variability. J Geophys Res 113:C03S90

Stammerjohn S, Massom R, Rind D, Martinson D (2012) Regions of rapid sea ice change: An inter-hemispheric seasonal comparison. Geophys Res Lett 39:L06501

Sweeting CJ, Polunin NVC, Jennings S (2006) Effects of chemical lipid extraction and arithmetic lipid correction on stable isotope ratios of fish tissues. Rapid Commun Mass Spectrom 20:595-601

Tortell PD, Payne CD, Li Y, Trimborn S, Rost B, Smith WO, Riesselman C, Dunbar RB, Sedwick P, DiTullio GR (2008) CO_2 sensitivity of Southern Ocean phytoplankton. Geophys Res Lett 35:L04605

Trathan PN, Forcada J, Murphy EJ (2007) Environmental forcing and Southern Ocean marine predator populations: effects of climate change and variability. Philos Trans R Soc Lond B Biol Sci 362:2351-2365

Ventura M (2006) Linking biochemical and elemental composition in freshwater and marine crustacean zooplankton. Mar Ecol Prog Ser 327:233-246

Villinski JC, Dunbar RB, Mucciarone DA (2000) Carbon 13/Carbon 12 ratios of sedimentary organic matter from the Ross Sea, Antarctica: A record of phytoplankton bloom dynamics. J Geophys Res, C, Oceans 105:14163-14172

Vokhshoori NL, Larsen T, McCarthy MD (2014) Reconstructing $\delta^{13}C$ isoscapes of phytoplankton production in a coastal upwelling system with amino acid isotope values of littoral mussels. Mar Ecol Prog Ser 504:59-72

Vokhshoori NL, McCarthy MD (2014) Compound-specific $\delta^{15}N$ amino acid measurements in littoral mussels in the California upwelling ecosystem: a new approach to generating baseline $\delta^{15}N$ isoscapes for coastal ecosystems. PLOS ONE 9:e98087

Wada E, Terazaki M, Kabaya Y, Nemoto T (1987) 15N and 13C abundances in the Antartic Ocean with emphasis on the biogeochemical structure of the food web. Deep Sea Res I 34:829-841

Wainwright SC, Fry B (1994) Seasonal variation of the stable isotopic compositions of coastal marine plankton from Woods Hole, Massachusetts and Georges Bank. Estuaries 17:552-560

Waser NA, Harrison WG, Head EJ, Nielsen B, Lutz VA, Calvert SE (2000) Geographic variations in the nitrogen isotope composition of surface particulate nitrogen and new production across the North Atlantic Ocean. Deep Sea Res I 47:1207-1226

West JB, Bowen GJ, Dawson TE, Tu KP (2010) Isoscapes. Springer, Netherlands

Yuan XI (2004) ENSO-related impacts on Antarctic sea ice: a synthesis of phenomenon and mechanisms. Antarct Sci 16:415-25

Zingone A, Phlips EJ, Harrison PJ (2010) Multiscale variability of twenty-two coastal phytoplankton time series: a global scale comparison. Estuar Coasts 33:224-229

922 **FIGURES**
923

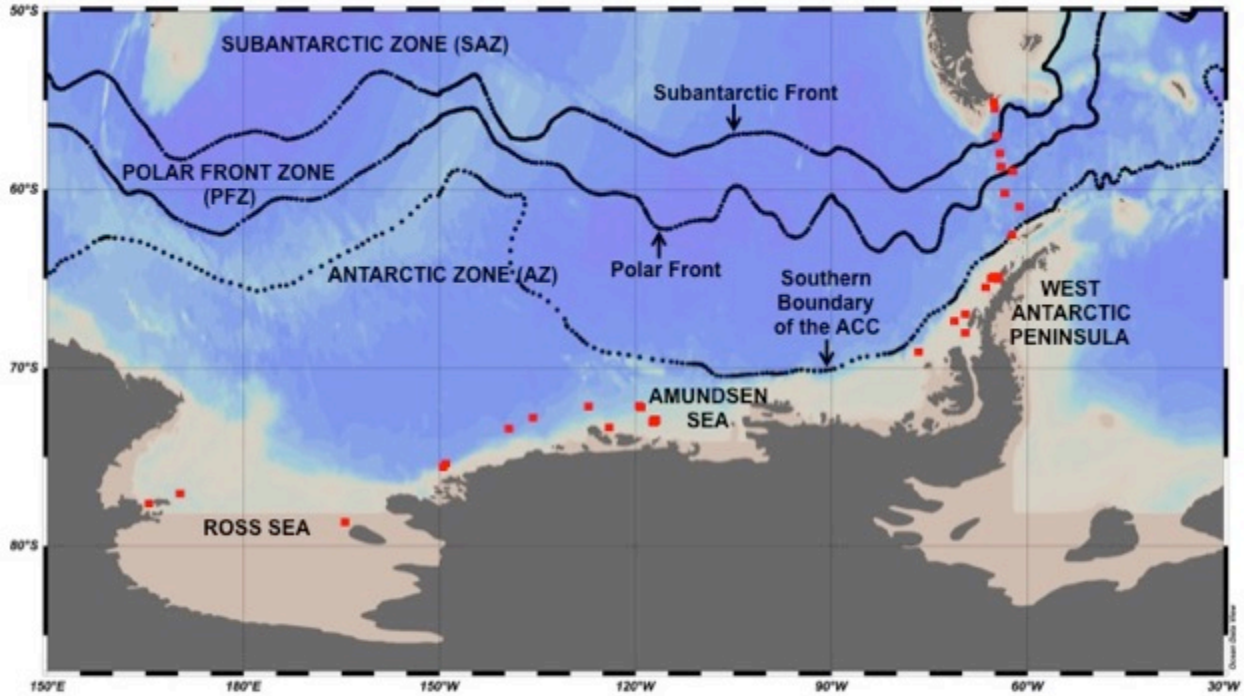

924
925 Fig 1. Zooplankton sampling locations for developing $\delta^{15}N$ and $\delta^{13}C$ isoscapes across five Southern Ocean
926 biogeographic zones. Major fronts are indicated with black dotted lines, according to Orsi et al. (1995). Red squares
927 represent sampling sites for zooplankton.

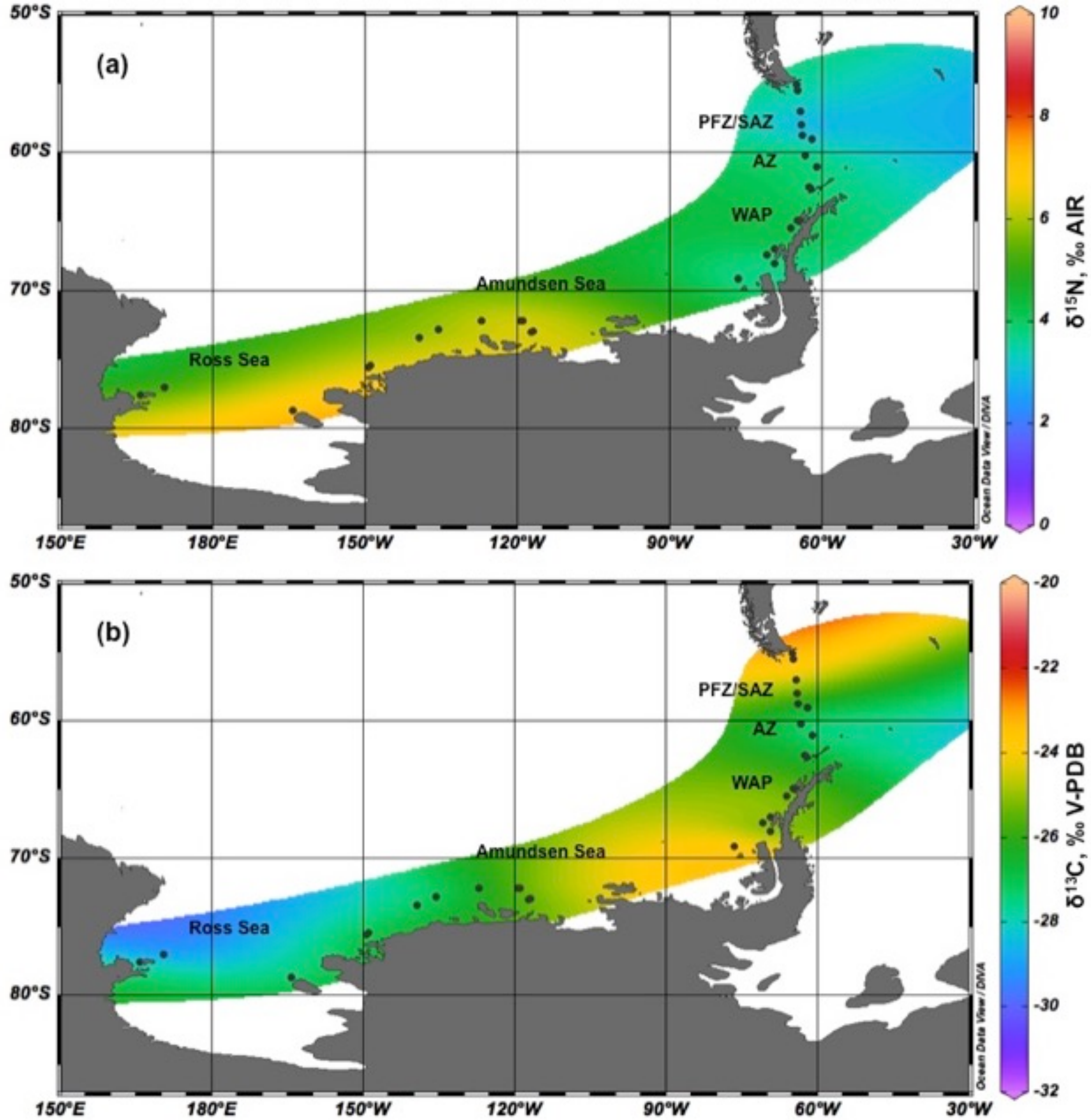

Fig. 2. δ^{15}N (a) and δ^{13}C (b) values (‰) of all zooplankton taxa from West Antarctica. These isoscapes include data for all zooplankton from all sampling periods. PFZ/SAZ, AZ, and WAP abbreviate Polar Front Zone/Subantarctic Zone, Antarctic Zone, and West Antarctic Peninsula, respectively. Isoscapes were produced in ODV 4.7.4 (Schlitzer 2015) using Data Interpolating Variational Analysis (DIVA) gridding software (Barth et al. 2010).

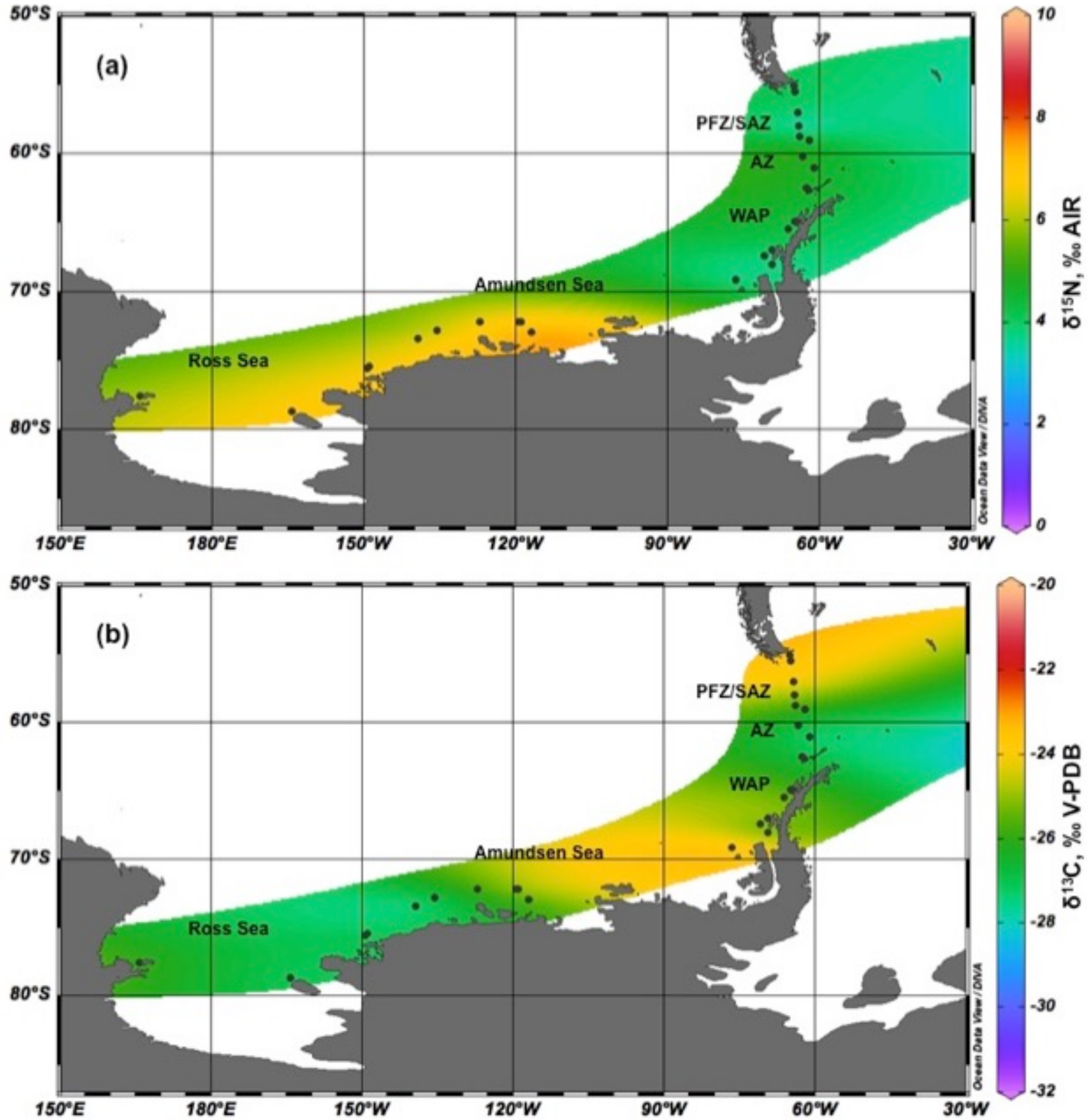

Fig. 3. $\delta^{15}N$ (a) and $\delta^{13}C$ (b) values (‰) of all euphausiids from West Antarctica. Euphausiid isoscapes include data from all sampling periods. PFZ/SAZ, AZ, and WAP abbreviate Polar Front Zone/Subantarctic Zone, Antarctic Zone, and West Antarctic Peninsula, respectively. Isoscapes were produced in ODV 4.7.4 (Schlitzer 2015) using Data Interpolating Variational Analysis (DIVA) gridding software (Barth et al. 2010).

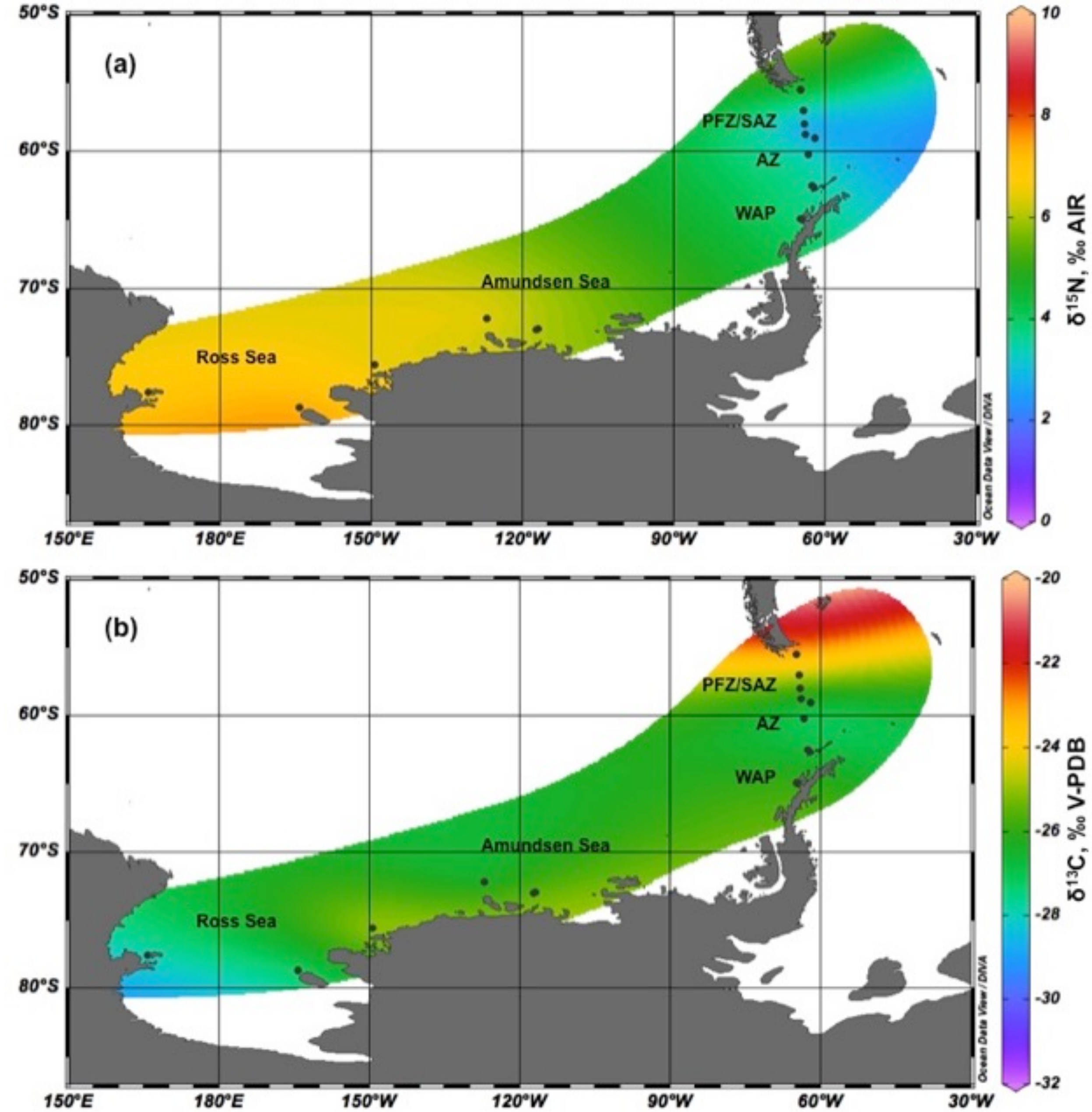

Fig. 4. $\delta^{15}N$ (a) and $\delta^{13}C$ (b) values (‰) of all amphipods from West Antarctica. Amphipod isoscapes include data from all sampling periods. PFZ/SAZ, AZ, and WAP abbreviate Polar Front Zone/Subantarctic Zone, Antarctic Zone, and West Antarctic Peninsula, respectively. Isoscapes were produced in ODV 4.7.4 (Schlitzer 2015) using Data Interpolating Variational Analysis (DIVA) gridding software (Barth et al. 2010).

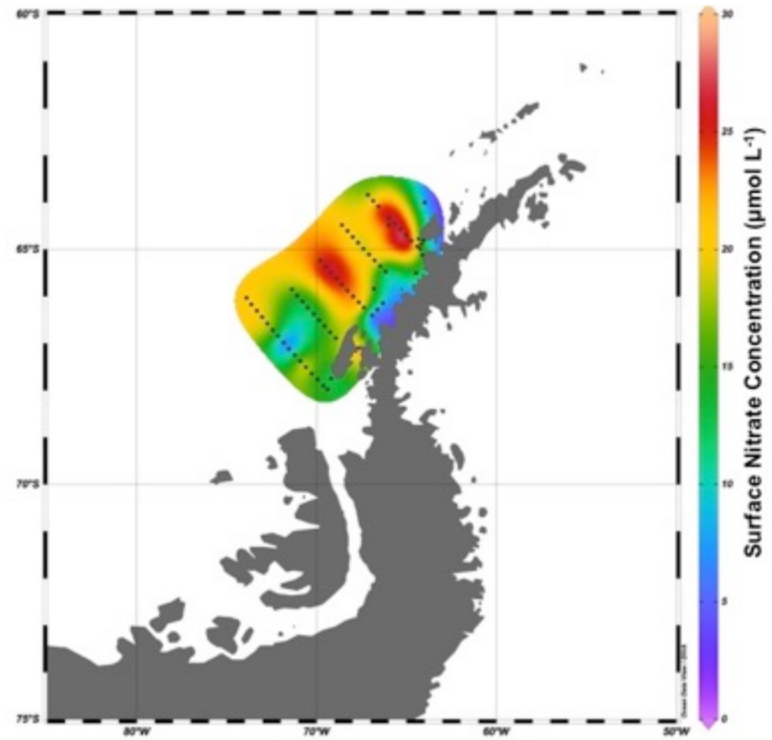

Fig. 5. Surface nitrate concentrations (μmol L^{-1}) off the WAP for the austral summer (January and February) of 2006, a time without a strong ENSO event. Plot produced in Ocean Data View 4.7.4 using a dataset from Ducklow et al. (2017a,b).

SUPPLEMENTAL MATERIAL

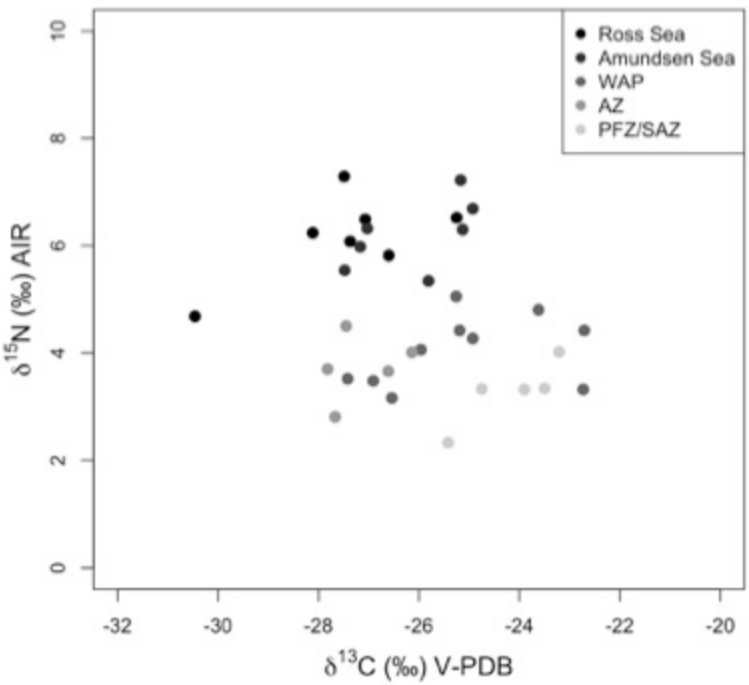

Fig. S1. δ^{15}N versus δ^{13}C values (‰) of zooplankton from West Antarctica. This figure includes data from all sampling periods. WAP, AZ, and PFZ/SAZ abbreviate West Antarctic Peninsula, Antarctic Zone, and Polar Front Zone/Subantarctic Zone, respectively.

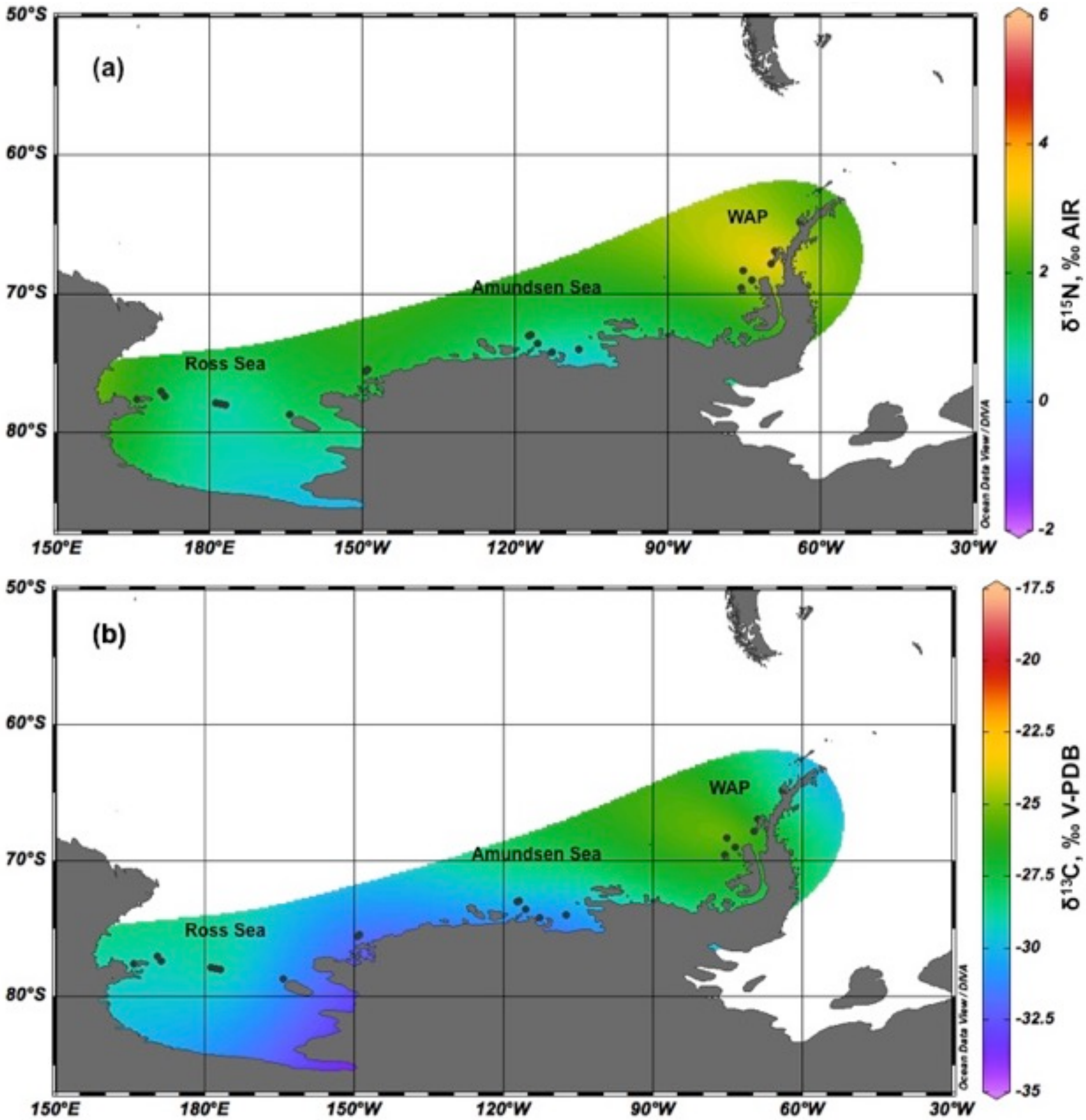

Fig. S2. δ^{15}N (a) and δ^{13}C (b) values (‰) of phytoplankton from West Antarctica. These isoscapes include data from all sampling periods. WAP abbreviates West Antarctic Peninsula. Isoscapes were produced in ODV 4.7.4 (Schlitzer 2015) using Data Interpolating Variational Analysis (DIVA) gridding software (Barth et al. 2010).

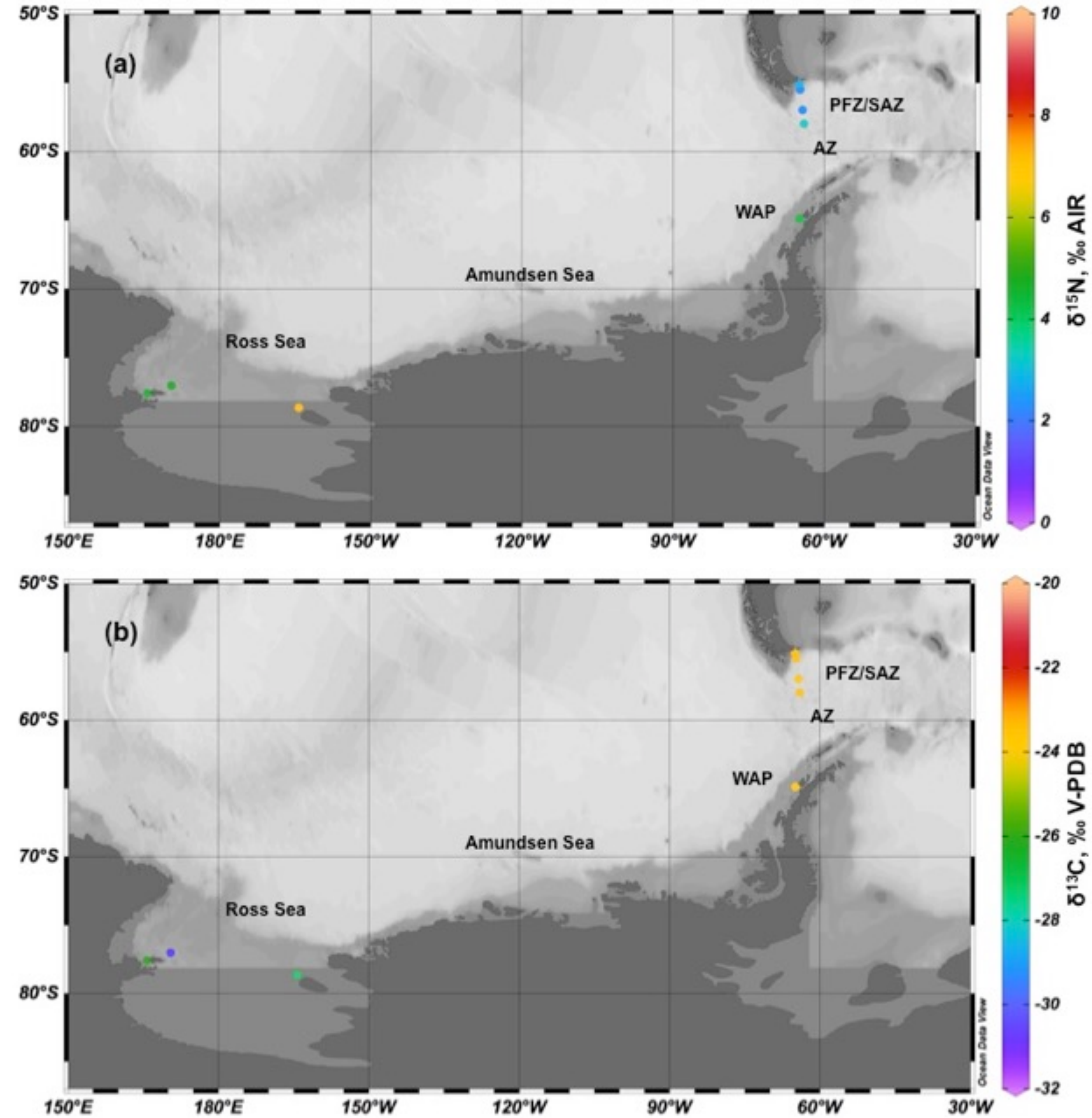

Fig. S3. $\delta^{15}N$ (a) and $\delta^{13}C$ (b) values (‰) of pteropods from West Antarctica. Pteropod isoscapes include data from all sampling periods. PFZ/SAZ, AZ, and WAP abbreviate Polar Front Zone/Subantarctic Zone, Antarctic Zone, and West Antarctic Peninsula, respectively. Isoscapes were produced in ODV 4.7.4 (Schlitzer 2015).

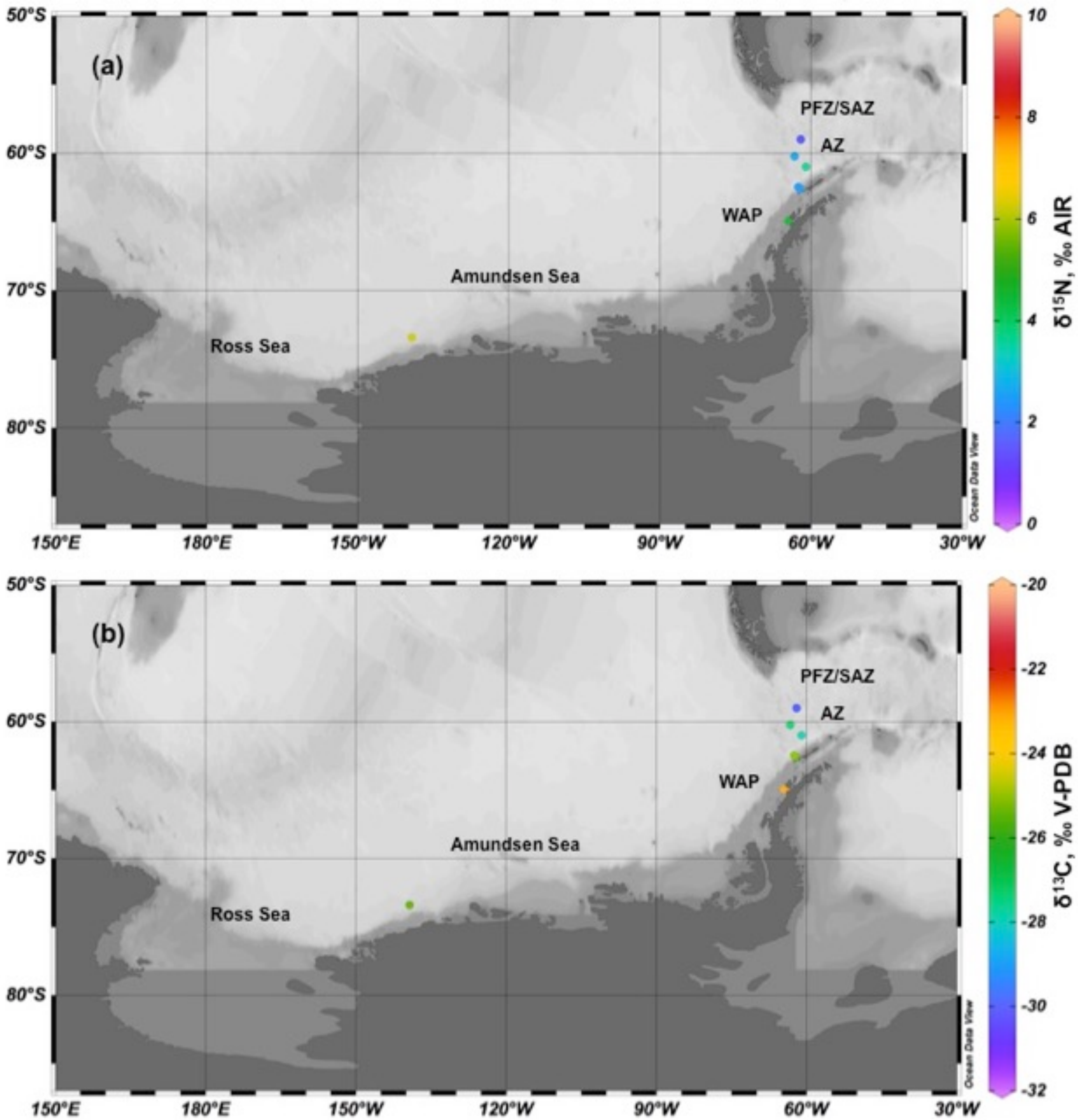

Fig. S4. $\delta^{15}N$ (a) and $\delta^{13}C$ (b) values (‰) of salps from West Antarctica. Salp isoscapes include data from all sampling periods. PFZ/SAZ, AZ, and WAP abbreviate Polar Front Zone/Subantarctic Zone, Antarctic Zone, and West Antarctic Peninsula, respectively. Isoscapes were produced in ODV 4.7.4 (Schlitzer 2015).

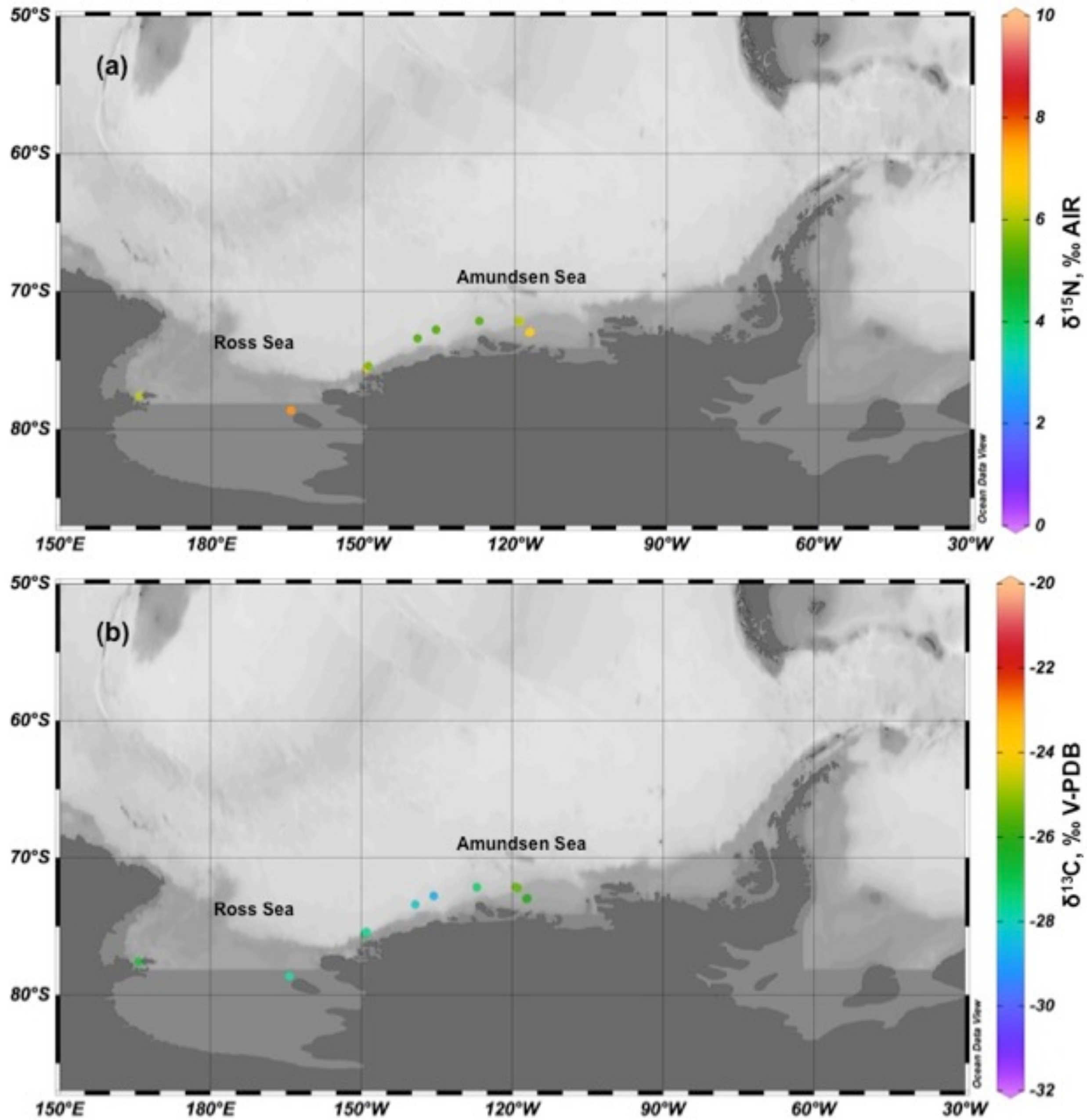

Fig. S5. $\delta^{15}N$ (a) and $\delta^{13}C$ (b) values (‰) of copepods from West Antarctica. Copepod isoscapes include data from all sampling periods. Isoscapes were produced in ODV 4.7.4 (Schlitzer 2015).

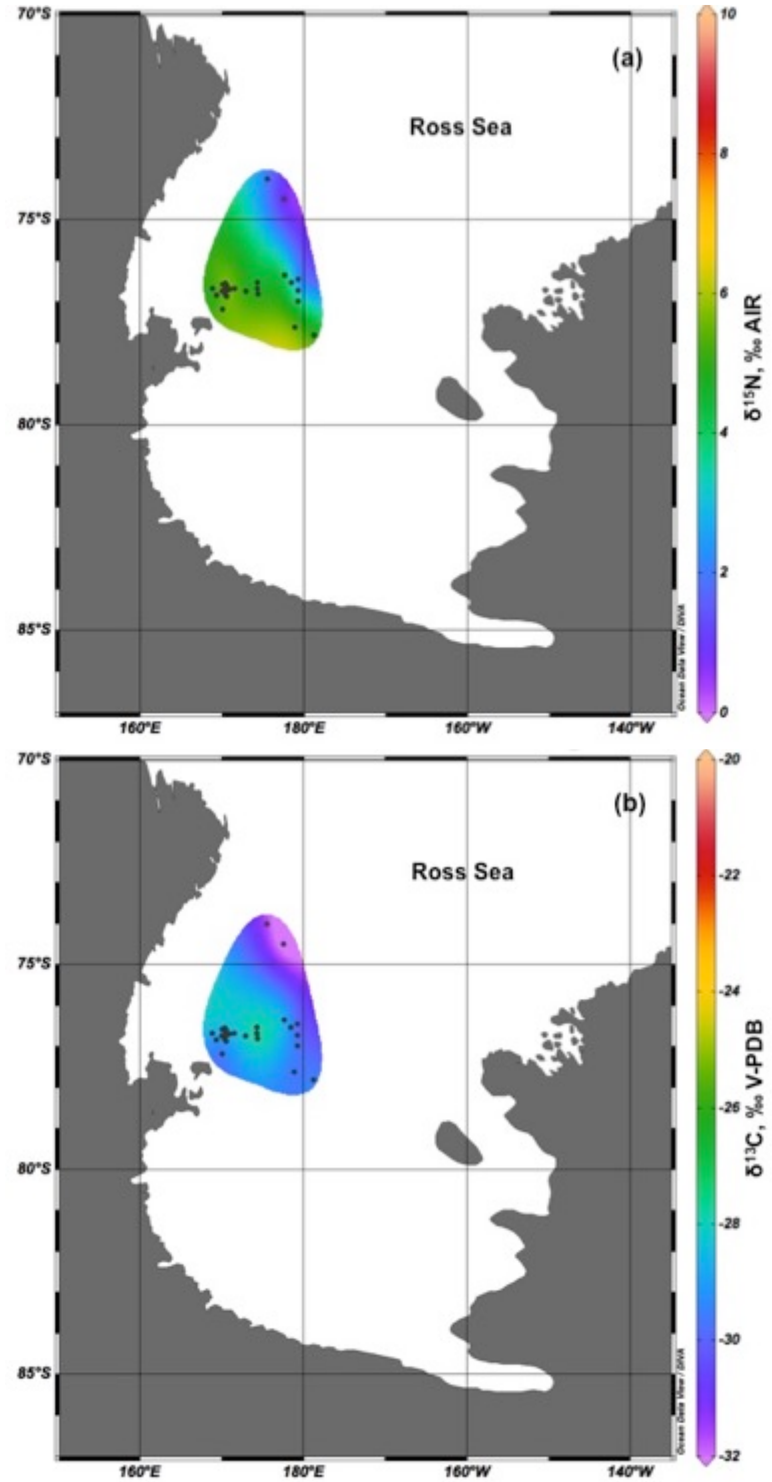

Fig. S6. $\delta^{15}N$ (a) and $\delta^{13}C$ (b) values (‰) of Ross Sea mixed, formalin-exposed plankton (0-200 µm). Mean ± standard deviation (sample size) for $\delta^{15}N$ and $\delta^{13}C$ are 4.7 ± 1.8 (27) and -29.0 ± 1.6 (27), respectively. Isoscapes were produced in ODV 4.7.4 (Schlitzer 2015) using Data Interpolating Variational Analysis (DIVA) gridding software (Barth et al. 2010).

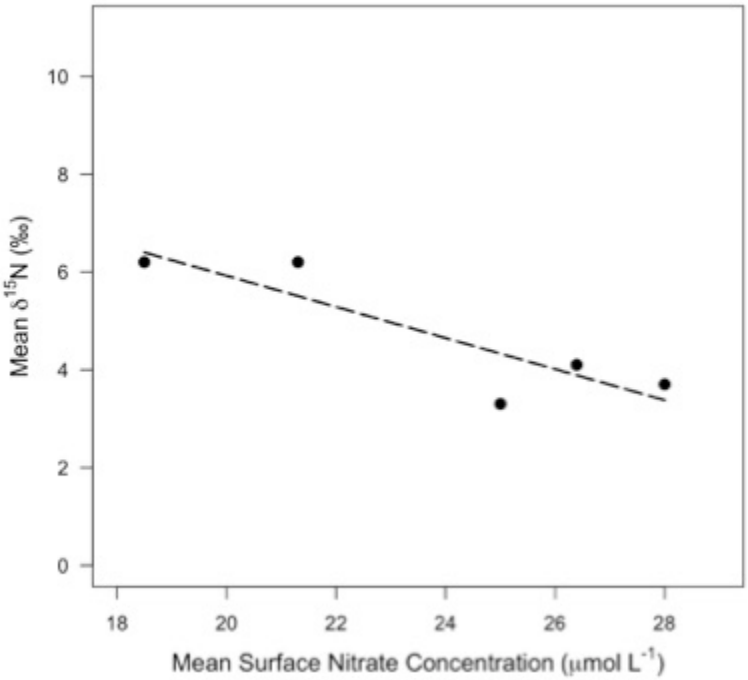

Fig. S7. Mean $\delta^{15}N$ values (‰) of all zooplankton taxa versus mean nitrate concentration (µmol L^{-1}) for their sampling region. Data from all sampling periods are shown.

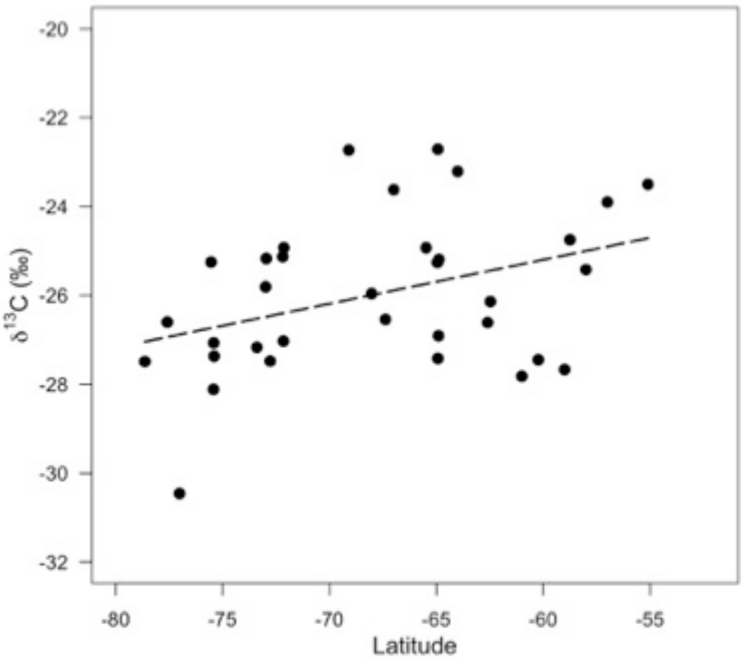

Fig. S8. $\delta^{13}C$ values (‰) of all zooplankton taxa versus latitude of sampling location. Data from all sampling periods are shown.

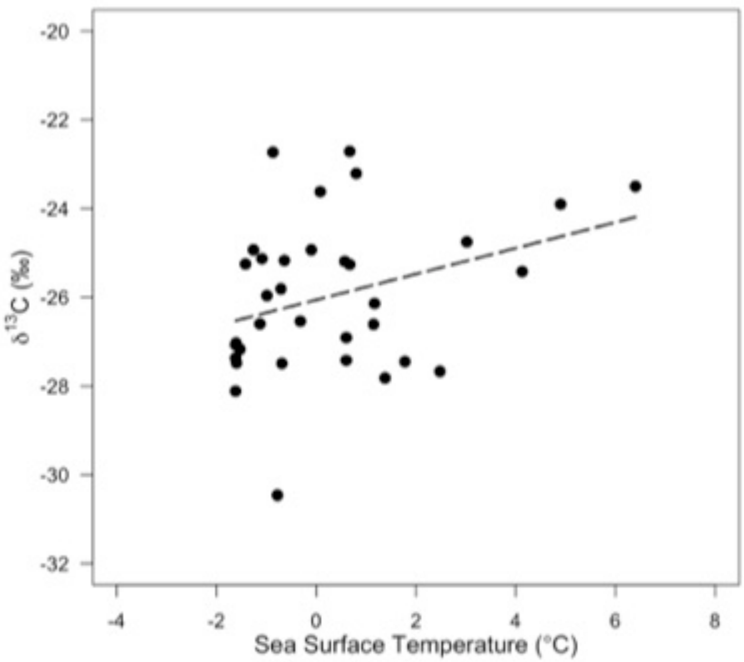

Fig. S9. $\delta^{13}C$ values (‰) of all zooplankton taxa versus sea surface temperature (°C) of sampling location. Data from all sampling periods are shown.

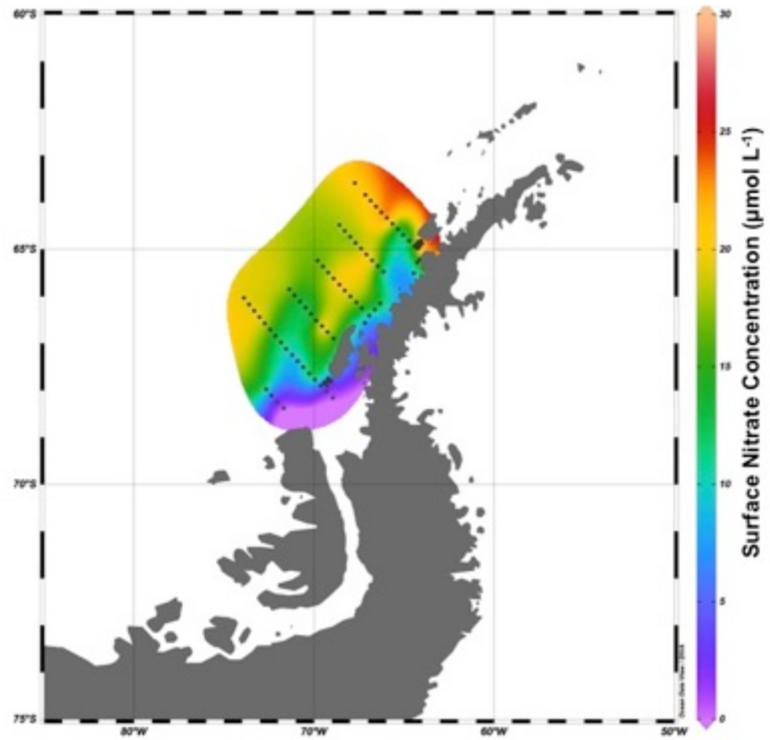

Fig. S10. Surface nitrate concentrations (µmol L^{-1}) off the WAP for austral summer (January and February) of 2007, which experienced El Niño conditions. Plot produced in Ocean Data View 4.7.4 using a dataset from Ducklow et al. (2017a,b).

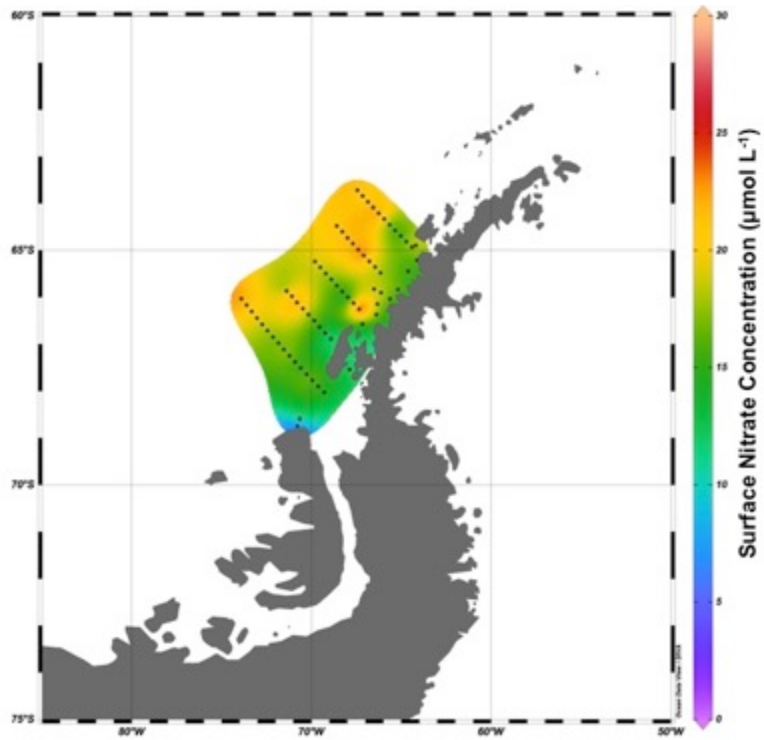

Fig. S11. Surface nitrate concentrations (µmol L^{-1}) off the WAP for austral summer (January and February) of 2008, which experienced strong La Niña conditions. Plot produced in Ocean Data View 4.7.4 using a dataset from Ducklow et al. (2017a,b).

Table S1. Isotopic data for all zooplankton. If multiple taxa were collected at a given site, then the mean ± standard deviation is reported for all zooplankton. *Su*, *Sp*, *E.*, *Amund*, *WAP*, *SST*, and *juv* abbreviate *Summer*, *Spring*, *Euphausia, Amundsen*, *West Antarctic Peninsula*, *Sea Surface Temperature*, and *juvenile*, respectively. Additionally, the years *2007*, *2008*, *2010*, *2011*, and *2015* are abbreviated as *07*, *08*, *10*, *11*, and *15*. The C:N ratios are atomic and reported for lipid-extracted material. SSTs derive from Gouretski and Koltermann (2004).

Region, Time	Lat (DD)	Long (DD)	$\delta^{13}C$ (‰)	$\delta^{15}N$ (‰)	C:N	SST (°C)	Taxa	Source
Amund Sea Su 10/11	-72.99	-117.19	-25.8±2.5	5.3±0.9		-0.7	All Zooplankton	This Study
			-26.1	6.3	4.1		Copepod	
			-23.1	4.6	7.0		Gammarid amphipod	
			-28.2	5.2	5.7		Hyperiid amphipod	
Amund Sea Su 10/11	-72.96	-116.97	-25.2±1.6	7.2±1.9		-0.6	All Zooplankton	This Study
			-26.2	6.9	4.0		Copepod	
			-22.8	4.7	7.3		Gammarid amphipod	
			-26.0	9.2	4.4		Hyperiid amphipod	
			-25.6	8.3	4.1		Euphausiid (larval)	
Amund Sea Su 10/11	-72.19	-118.96	-25.1±0.6	6.3±0.1		-1.1	All Zooplankton	This Study
			-25.6	6.2	3.9		Copepod	
			-24.7	6.4	4.3		Euphausiid (larval)	
Amund Sea Su 10/11	-72.14	-119.32	-24.9±0.6	6.7±0.9		-1.3	All Zooplankton	This Study
			-25.4	6.1	3.8		Copepod	
			-24.5	7.3	4.2		Euphausiid (larval)	
Amund Sea Su 10/11	-72.16	-127.08	-27.0±1.0	6.3±0.8		-1.6	All Zooplankton	This Study
			-27.4	5.4	4.3		Copepod	
			-27.8	6.9	5.3		Hyperiid amphipod	
			-25.9	6.6	–		Euphausiid (larval)	
Amund Sea Su 10/11	-72.78	-135.59	-27.5±2.0	5.5±0.2		-1.6	All Zooplankton	This Study
			-28.6	5.4	4.0		Copepod	
			-28.6	5.8	4.2		Euphausiid (larval)	
			-25.2	5.4	4.1		Euphausiid (adult)	
Amund Sea Su 10/11	-73.40	-139.28	-27.2±1.5	6.0±0.5		-1.5	All Zooplankton	This Study
			-28.2	5.4	4.3		Copepod	
			-27.9	6.3	4.8		Euphausiid (larval)	
			-25.4	6.2	3.8		*Salpa thomsoni*	
Ross Sea Su 10/11	-75.40	-149.00	-27.4±0.6	6.1±0.0		-1.6	All Zooplankton	This Study
			-27.8	6.1	3.7		Copepod	
			-26.9	6.1	4.2		Euphausiid (juv)	
Ross Sea Su 10/11	-75.42	-149.00	-27.1±0.3	6.5±0.6		-1.6	All Zooplankton	This Study
			-27.4	6.3	4.4		Copepod	
			-26.9	7.2	4.2		Euphausiid (larval)	
			-26.9	6	4.3		Euphausiid (juv)	
Ross Sea Su 10/11	-75.43	-149.01	-28.1±0.5	6.2±0.8		-1.6	All Zooplankton	This Study
			-27.8	5.7	4.1		Copepod	
			-28.5	6.8	4.6		Euphausiid (larval)	
Ross Sea Su 07/08	-77.02	170.46	-30.5	4.7	8.4	-0.8	*Clione limacina*	This Study
Ross Sea Su 10/11 Summer 2007/08	-75.54	-149.30	-25.3±2.5	6.5±1.3		-1.4	All Zooplankton	This Study
			-26.8	6.7	4.1		Copepod	
			-21.1	4.8	8.3		Gammarid amphipod	
			-26.5	7.6	4.7		Hyperiid amphipod	
			-27.2	5.7	4.2		Euphausiid (juv)	
			-24.7	7.8	4.5		Euphausiid (adult)	
Ross Sea Su 10/11	-78.64	-164.3	-27.5±0.4	7.3±0.6		-0.7	All Zooplankton	This Study
			-27.7	7.6	4.3		Copepod	

			-27.9	7.9	5.6		Gammarid amphipod	
			-27.9	7.6	4.5		Hyperiid amphipod	
			-27.4	7.4	4.2		Euphausiid (larval)	
			-27.0	6.2	4.1		Euphausiid (juv)	
			-26.8	7.7	4.8		*Clione limacina*	
			-27.8	6.6	6.8		*Limacina helicina*	
Ross Sea Su 10/11	-77.59	165.71	-26.6±1.1	5.8±1.1		-1.1	All Zooplankton	This Study
			-26.8	6.1	4.0		Copepod	
			-28.1	6.6	8.5		Gammarid amphipod	
			-27.5	7.2	6.3		Hyperiid amphipod	
			-26.1	6.5	4.1		Euphausiid (larval)	
			-25.4	5.4	4.1		Euphausiid (juv)	
			-25.3	4.9	4.3		*Clione limacina*	
			-26.9	4.2	6.3		*Limacina helicina*	
AZ Sp 15	-61.00	-61.00	-27.8±0.2	3.7±0.2		-1.4	All Zooplankton	This Study
			-27.7	3.8	4.3		*Euphausia superba*	
			-27.9	3.6	5.3		*Salpa thomsoni*	
WAP Sp 15	-64.88	-64.90	-25.2±1.7	4.4±1.7		-0.6	All Zooplankton	This Study
			-26.1	4.0	4.2		*E. superba*	
			-23.1	5.6	4.1		*E. crystallorophias*	
			-27.2	6.4	4.7		*Thysanoessa macrura*	
			-25.8	1.9	4.5		*Themisto gaudichaudii*	
			-23.7	4.2	4.4		*Spongiobrachia australis*	
WAP Sp 15	-64.95	-64.43	-25.3±1.5	5.1±1.0		-0.7	All Zooplankton	This Study
			-26.7	4.0	4.3		*E. superba*	
			-25.7	6.0	4.3		*Thysanoessa macrura*	
			-25.6	5.7	4.4		*Themisto gaudichaudii*	
			-23.1	4.5	5.2		*Salpa thomsoni*	
AZ Sp 15	-62.60	-62.02	-26.6±0.6	3.7±0.9		1.2	All Zooplankton	This Study
			-26.6	3.5	3.9		*E. superba*	
			-27.1	5.1	4.6		*Thysanoessa macrura*	
			-26.6	3.4	4.6		*Vibilia antarctica*	
			-27.2	3.8	4.7		*Themisto gaudichaudii*	
			-25.7	2.5	4.9		*Salpa thomsoni*	
AZ Sp 15	-62.47	-62.47	-26.1±0.8	4.0±1.2		1.2	All Zooplankton	This Study
			-26.0	5.0	4.1		*E. frigida*	
			-27.1	5.3	4.5		*Thysanoessa macrura*	
			-26.3	3.6	4.7		*Vibilia antarctica*	
			-26.4	3.6	4.4		*Themisto gaudichaudii*	
			-25.0	2.5	4.8		*Salpa thomsoni*	
AZ Sp 15	-60.23	-63.27	-27.5±0.8	4.5±2.2		1.8	All Zooplankton	This Study
			-26.8	6.2	4.2		*Thysanoessa macrura*	
			-28.5	2.5	4.6		*Vibilia antarctica*	
			-27.1	6.6	4.5		*Themisto gaudichaudii*	
			-27.5	2.7	5.4		*Salpa thomsoni*	
AZ Sp 15	-59.00	-62.00	-27.7±1.5	2.8±1.7		2.5	All Zooplankton	This Study
			-26.5	4.0	4.1		*E. frigida*	
			-26.6	5.1	4.1		*E. triacantha*	
			-28.3	2.6	5.1		*Vibilia antarctica*	
			-27.1	0.9	4.5		*Themisto gaudichaudii*	
			-29.9	1.6	5.7		*Salpa thomsoni*	
PFZ/ SAZ	-58.75	-63.78	-24.8±0.2	3.3±0.8		3.0	All Zooplankton	This Study
			-24.5	4.0	3.9		*E. triacantha*	

Sp 15			-25.0 -24.7	3.4 2.5	4.8 4.3		*Vibilia antarctica* *Themisto gaudichaudii*	
PFZ/ SAZ Sp 15	-58.00	-64.00	-25.4±2.0 -25.2 -28.8 -24.4 -25.0 -23.6	2.3±0.7 2.1 1.8 1.6 2.9 3.2	 4 5.3 4.4 4.4 4.5	4.1	All Zooplankton *E. triacantha* *Vibilia antarctica* *Primno macropa* *Themisto gaudichaudii* *Spongiobrachia australis*	This Study
PFZ/ SAZ Sp 15	-57.00	-64.33	-23.9±0.4 -23.4 -24.4 -24.0 -23.8	3.3±1.1 4.6 2.4 3.9 2.4	 4.1 4.4 4.5 4.4	4.9	All Zooplankton *E. triacantha* *Primno macropa* *Themisto gaudichaudii* *Spongiobrachia australis*	This Study
PFZ/ SAZ Sp 15	-64.00	-64.80	-23.2±0.7 -23.7 -22.5 -23.5	4.0±1.6 4.4 5.4 2.3	 4.1 4.3 4.3	0.8	All Zooplankton *E. triacantha* *Themisto gaudichaudii* *Spongiobrachia australis*	This Study
PFZ/ SAZ Sp 15	-55.1	-64.95	-23.5±0.0 -23.5 -23.5	3.3±0.8 3.9 2.8	 4.1 4.2	6.4	All Zooplankton *E. triacantha* *Spongiobrachia australis*	This Study
WAP Su 07/08	-66.99	-69.28	-23.6±1.2 -22.6 -22.8 -23.9 -25.2	4.8±0.5 5.0 5.1 5.1 4.0	 3.9 4.0 4.1 4.0	4.8	All Zooplankton *E. superba* (gravid) *E. superba* (mature females) *E. superba* (adults) *E. superba* (juv)	Brault (2012)
WAP Su 07/08	-64.90	-64.18	-26.9	3.5	4.2	3.5	*E. superba* (adults)	Brault (2012)
WAP Su 07/08	-68.03	-69.28	-26.0	4.1	4.0	4.1	*E. superba* (adults)	Brault (2012)
WAP Su 07/08	-64.93	-64.25	-27.4±0.2 -27.3 -27.6	3.5±0.0 3.5 3.5	 4.2 3.9	3.5	All Zooplankton *E. superba* (adults) *E. superba* (juv)	Brault (2012)
WAP Su 10/11	-69.10	-76.45	-22.7	3.3	4.2	3.3	*E. superba* (gravid)	Brault (2012)
WAP Su 10/11	-64.93	-64.40	-22.7	4.4	4.2	4.4	*E. superba* (juv)	Brault (2012)
WAP Su 10/11	-65.48	-66.15	-24.9	4.3	4.0	4.3	*E. superba* (adults)	Brault (2012)
WAP Su 07/08	-67.38	-70.91	-26.5	3.2	4.2	3.2	*E. superba* (adults)	Brault (2012)

Table S2. Isotopic values (‰) of formalin-exposed plankton (0-200 µm) from the Ross Sea. $\delta^{13}C$ and $\delta^{15}N$ values of all plankton measured.

Sample ID	Latitude (DD)	Longitude (DD)	$\delta^{13}C$ (‰)	$\delta^{15}N$ (‰)	C:N (Atomic)
Phyt_38	-76.72	179.26	-30.8	0.5	6.6
Phyt_92	-74.50	177.50	-33.2	0.2	7.1
Phyt_19	-76.74	172.88	-28.1	4.6	6.2
Phyt_26	-76.80	174.30	-27.0	4.9	5.9
Phyt_105	-76.57	170.00	-27.8	5.3	6.6
Phyt_42	-76.34	177.62	-27.1	5.6	4.9
Phyt_10	-76.73	170.48	-28.0	5.5	7.6
Phyt_110	-77.17	170.00	-29.9	6.2	6.4
Phyt_113	-76.84	169.30	-30.8	2.8	6.7
Phyt_12	-76.73	169.89	-29.9	6.0	6.6
Phyt_14	-76.73	170.06	-28.1	6.2	6.1
Phyt_15	-76.86	170.47	-28.2	4.4	6.3
Phyt_18	-76.60	170.48	-28.4	5.9	6.9
Phyt_22	-76.53	174.25	-28.4	4.2	5.7
Phyt_27	-76.81	170.33	-31.0	6.3	7.6
Phyt_29	-76.68	170.33	-27.0	5.6	6.0
Phyt_31	-76.55	170.33	-29.5	6.3	6.6
Phyt_35	-76.68	170.91	-29.3	6.3	7.9
Phyt_40	-76.53	178.43	-29.2	5.4	6.2
Phyt_44	-76.45	179.25	-30.3	0.8	7.8
Phyt_48	-76.98	179.25	-29.0	5.2	6.0
Phyt_56	-77.80	-178.80	-29.0	5.2	5.8
Phyt_65	-77.61	178.80	-30.3	5.8	6.7
Phyt_7	-76.67	168.78	-26.9	5.3	5.7
Phyt_8	-76.67	171.50	-28.2	5.5	5.9
Phyt_89	-74.00	175.49	-31.4	2.5	6.6
Phyt_9	-76.67	174.25	-27.6	4.4	5.6

Table S3. Surface nitrate concentrations (μmol L^{-1}) determined for West Antarctic regions. *PFZ/SAZ*, *AZ*, and *WAP* abbreviate *Polar Front Zone, Subantarctic Zone*, and *Antarctic Zone*, respectively.

Surface Nitrate Concentrations (μmol L^{-1})	**Region**	**Season**	**Source**
22.0	PFZ/SAZ	Summer	Sanders and Jickells (2009)
28.0	AZ	Summer	Sanders and Jickells (2009)
24.7	WAP	Summer	Ducklow et al. (2017)
14.6	Amundsen Sea	Summer	Alderkamp et al. (2012)
9.0	Ross Sea	Summer	Gordon et al. (2000), Sweeney et al. (2000)
28.0	PFZ/SAZ	Spring	DiFiore et al. (2006), Clarke et al. (2008)
28.0	AZ	Spring	DiFiore et al. (2006), Clarke et al. (2008)
28.0	WAP	Spring	Clarke et al. (2008)
28.0	Amundsen Sea	Spring	Gordon et al. (2000), Sweeney et al. (2000)
28.0	Ross Sea	Spring	Gordon et al. (2000), Sweeney et al. (2000)

Table S4. Isotopic values of phytoplankton. $\delta^{13}C$ and $\delta^{15}N$ values of all phytoplankton sampled during various field seasons for three Antarctic regions (WAP, Amundsen Sea, and Ross Sea). Isotopic data are reported as mean ± standard deviation (sample size).

Region	$\delta^{13}C$ (‰)			$\delta^{15}N$ (‰)		
	2007/08	2009/10	2010/11	2007/08	2009/10	2010/11
WAP	–	-30.2 ± 3.3 (3)	-25.0 ± 5.7 (5)	–	1.8 ± 0.8 (3)	3.4 ± 1.8 (5)
Amundsen Sea	-31.5 ± 0.9 (4)	–	-28.2 ± 0.8 (2)	0.3 ± 0.6 (4)	–	1.9 ± 0.1 (2)
Ross Sea	-28.8 ± 3.3 (7)	–	-31.1 ± 1.8 (5)	0.9 ± 1.4 (7)	–	2.0 ± 0.6 (5)